



UNIVERSIDAD DE INVESTIGACIÓN DE TECNOLOGÍA EXPERIMENTAL YACHAY

Escuela de Ciencias Físicas y Nanotecnología

TÍTULO: Interior Solutions by Gravitational Decoupling

Trabajo de integración curricular presentado como requisito para la
obtención del título de Físico

Autor:

Coello Villalta Cristhian Enrique

Tutor:

M.Sc. – David Andrade Acosta

Cotutor:

M.Sc. – Julio Andrade Landeta

Urququí, enero 2024

Autoría

Yo, **Cristhian Enrique Coello Villalta**, con cédula de identidad 1150678520, declaro que las ideas, juicios, valoraciones, interpretaciones, consultas bibliográficas, definiciones y conceptualizaciones expuestas en el presente trabajo; así cómo, los procedimientos y herramientas utilizadas en la investigación, son de absoluta responsabilidad de el/la autor/a del trabajo de integración curricular. Así mismo, me acojo a los reglamentos internos de la Universidad de Investigación de Tecnología Experimental Yachay.

Urcuquí, enero 2024.

Cristhian Enrique Coello Villalta

CI: 1150678520

Autorización de publicación

Yo, **Cristhian Enrique Coello Villalta**, con cédula de identidad 1150678520, cedo a la Universidad de Investigación de Tecnología Experimental Yachay, los derechos de publicación de la presente obra, sin que deba haber un reconocimiento económico por este concepto. Declaro además que el texto del presente trabajo de titulación no podrá ser cedido a ninguna empresa editorial para su publicación u otros fines, sin contar previamente con la autorización escrita de la Universidad.

Asimismo, autorizo a la Universidad que realice la digitalización y publicación de este trabajo de integración curricular en el repositorio virtual, de conformidad a lo dispuesto en el Art. 144 de la Ley Orgánica de Educación

Urcuquí, enero 2024.

Cristhian Enrique Coello Villalta

CI: 1150678520

Dedication

I dedicate this first work to my entire family. Specially, to my loving parents Herman and Louricia; thanks to all their love, time and devotion that helped me persevere in the career, and made this possible. Their legacy will live forever with me. Additional thanks to my friends, professors, tutor and all people who supported me.

Cristhian Enrique Coello Villalta

Acknowledgment

An Important acknowledgment to my advisor M.Sc. David Andrade for all his support, time and guidance in encouraging me to finish this work. His marvelous ideas, enormous willingness and abnegated performance bequeath me the necessary knowledge and power to make this work possible.

My sincere thanks to all my professors and friends who supported me during the process, patiently shared their experience, and helped me in difficult times. Finally, to my co-advisor M.Sc. Julio Andrade for granting me his time and knowledge, necessary to complete my research.

Cristhian Enrique Coello Villalta

Resumen

Investigamos la introducción de anisotropía dentro de la solución de un fluido perfecto mediante el método de deformación geométrica mínima simple (MGD). La técnica nos permite incorporar una deformación en una solución previamente obtenida llamada semilla, luego, al desacoplar la ECE (Ecuaciones de Campo de Einstein) en dos sistemas, podemos buscar los componentes de esta perturbación. La semilla utilizada en este trabajo fue el sistema isotrópico resultado de la aplicación del método MGD extendido, proporcionado por J. Andrade (2022); la llamada solución Andrade-Einstein. Implementamos el MGD y obtuvimos una solución anisotrópica original. Consecutivamente, para completar el nuevo sistema, emparejamos dos soluciones en la frontera del sistema, una externa dispuesta por la tradicional métrica de Schwarzschild, y una interna dada por el nuevo resultado obtenido. La solución obtenida cumplió todas las condiciones de aceptabilidad física, convirtiéndose en un modelo adecuado para objetos estelares cuya compacidad se encuentra dentro del intervalo $[0,1, 0,16]$.

Palabras Clave:

Desacoplamiento Gravitacional, Deformación Geométrica Mínima, Solución Semilla, Relatividad General.

Abstract

We investigated the introduction of anisotropy inside the perfect fluid solution by the simple Minimal Geometric Deformation (MGD) approach. The technique enables us to embed a deformation into a previously obtained solution called seed, then by decoupling the EFE into two systems, we can search for the components of this perturbation. The seed utilized in this work was the isotropic outcome system from applying the extended MGD method, provided by J. Andrade in a recent paper (2022); the so-called Andrade-Einstein solution. We implemented the MGD, and elicited an original anisotropic solution. Consecutively, to complete the new system, we matched two solutions at the boundary of the system, an external one disposed by the traditional Schwarzschild metric, and an internal one given by the new attained result. The gained solution fulfilled all the physical acceptability conditions becoming a suitable model for stellar objects which compactness u lays inside the interval $[0.1, 0.16]$.

Keywords:

Gravitational Decoupling, Minimal Geometric Transformation, Seed Solution, General Relativity

Contents

Dedication	iii
Acknowledgment	iv
Resumen	v
Abstract	vi
Contents	vii
List of Figures	ix
1 Introduction	1
1.1 Problem statement	2
1.2 Objectives	3
1.2.1 General Objective	3
1.2.2 Specific Objectives	3
2 General Relativity	5
2.1 General Relativity	5
2.2 Manifolds in Differential Geometry	6
2.2.1 Riemannian and pseudo-Riemannian Manifolds	8
2.3 Einstein Field Equations (EFE)	9
2.3.1 The Riemann Tensor and Curvature	10
2.3.2 Energy-Stress Tensor and Fluid Motion	12
2.3.3 The Field Equations from Riemann Geometry	13
2.4 Fundamental Solutions	14
2.4.1 Einstein Static Universe Solution	16

2.4.2	Schwarzschild-de-Sitter Solution	16
2.4.3	Tolman IV Solution	17
3	Methodology	19
3.1	Minimal Geometric Deformation by Gravitational Decoupling	19
3.1.1	Gravitational Decoupling of Einstein Field Equations	22
3.1.2	External Metric and Matching Conditions	26
3.1.3	Complete System of Equations: The Constrains	28
3.2	Physical Acceptability Conditions	30
3.3	Introducing the Andrade-Einstein solution	33
4	Results and Discussion	36
4.1	The New Solution	36
4.2	Physical Analysis of the Solution	42
5	Conclusions	53
	Bibliography	55

List of Figures

2.1	Mapping: $(M \rightarrow R^n)$ from Manifold to Euclidean Space	7
2.2	Curved space-time due to the presence of mass-energy (stellar object). Image source: https://uh.edu/~protect/unhbox/voidb@x/protect/penalty/@M\{}jclarage/astr3131/lectures/4/einstein/Einstein_stanford_Page7.html	9
2.3	Parallel Transport of a first-rank tensor around a closed loop	10
3.1	MGD as an extension of General Relativity.	20
4.1	New Temporal Metric Component e^ν , $\alpha = 0.3$ for different values of compactness ($u = 0.1$ black, $u = 0.15$ blue, $u = 0.2$ red, $u = 0.3$ green)	42
4.2	New Radial Metric Component $\mu = e^{-\lambda}$, $\alpha = 0.3$ for different values of compactness ($u = 0.1$ black, $u = 0.15$ blue, $u = 0.2$ purple, $u = 0.3$ red) . .	43
4.3	The Effective density $\tilde{\rho}$, $\alpha = 0.3$ for different values of compactness ($u = 0.1$ black, $u = 0.15$ blue, $u = 0.2$ purple, $u = 0.3$ red).	44
4.4	The radial component of pressure \tilde{p}_r , $\alpha = 0.3$ for different values of compactness ($u = 0.1$ black, $u = 0.15$ blue, $u = 0.2$ purple, $u = 0.3$ red).	44
4.5	The tangential component of pressure (shear stress) \tilde{p}_t , $\alpha = 0.3$ for different values of compactness ($u = 0.1$ black, $u = 0.15$ blue, $u = 0.2$ purple, $u = 0.3$ red).	45
4.6	Dominant Energy Condition (DEC) for radial pressure $\rho(r) - p_r(r)$, $\alpha = 0.3$ for different values of compactness ($u = 0.1$ black, $u = 0.15$ blue, $u = 0.2$ purple, $u = 0.3$ red).	46

4.7	Dominant Energy Condition (DEC) for tangential pressure $\rho(r) - p_t(r)$, $\alpha = 0.3$ for different values of compactness ($u = 0.1$ black, $u = 0.15$ blue, $u = 0.2$ purple, $u = 0.3$ red).	46
4.8	The Strong Energy condition (SEC) $\rho - p_r - 2p_t$, $\alpha = 0.3$ for different values of compactness ($u = 0.1$ black, $u = 0.15$ blue, $u = 0.2$ purple, $u = 0.3$ red).	47
4.9	The Surface Redshift Z_s , $\alpha = 0.3$ for different values of compactness ($u = 0.1$ black, $u = 0.15$ blue, $u = 0.2$ purple, $u = 0.3$ red).	47
4.10	The Redshift $Z(r)$, $\alpha = 0.3$ for different values of compactness ($u = 0.1$ black, $u = 0.15$ blue, $u = 0.2$ purple, $u = 0.3$ red).	48
4.11	The Anisotropy of the system $\Pi = \tilde{p}_t - \tilde{p}_r$, $\alpha = 0.3$ for different values of compactness ($u = 0.1$ black, $u = 0.15$ blue, $u = 0.2$ purple, $u = 0.3$ red).	49
4.12	The radial component of sound speed v_r/c , $\alpha = 0.3$ for different values of compactness ($u = 0.1$ black, $u = 0.2$ blue, $u = 0.3$ purple, $u = 0.4$ red). The dashed-gray line represents the upper limit c	49
4.13	The tangential component of sound speed v_t/c , $\alpha = 0.3$ for different values of compactness ($u = 0.1$ black, $u = 0.2$ blue, $u = 0.3$ purple, $u = 0.4$ red). The dashed-gray line represents the upper limit c	50
4.14	Stability against cracking $v_t^2 - v_r^2$, $\alpha = 0.3$ for different values of compactness ($u = 0.1$ black, $u = 0.15$ blue, $u = 0.2$ purple, $u = 0.3$ red).	51
4.15	Adiabatic Factor Γ , $\alpha = 0.3$ for different values of compactness ($u = 0.1$ black, $u = 0.15$ blue, $u = 0.2$ purple, $u = 0.3$ red). The dashed-gray line represents the lower limit $\frac{4}{3}$	51

Chapter 1

Introduction

General Relativity (GR) stands as a marvelous and remarkable achievement within the realm of physical theories, empowering scientists to elucidate one of the most fundamental forces in the cosmos: gravity. Its capacity to exhibit how the presence of matter-energy can warp the fabric of space-time is unbelievable. The framework of General Relativity draws upon a spectrum of tools, starting within the branch of Differential Geometry to the somewhat laborious yet powerful Tensor Analysis. The beauty of GR concedes us an effective apparatus to unveil the working mechanics of many phenomena such as stellar objects, black holes, galaxies and the Universe itself [1].

Albert Einstein published his theory of General Relativity in 1915 as an extension of special relativity proposed by himself in 1905. Some experiments have demonstrated the validity of the theory; between them we have: The precession of Mercury's perihelion [2], the deflection of light by the Sun's gravitational field, the gravitational Redshift of galaxies, the LIGO experiment of gravitational waves [3], and the recent image of a black hole [3]. The study of gravitational fields in GR is also theoretical. Physicists have just elucidated a few forms of solving the mathematical machinery inside the Einstein Equations in order to find applied models for different gravitational phenomena.

The equations that govern all the General Relativity are called Einstein Field Equations (E.F.E). This is a system of differential equations that relates the properties of matter-energy and their transformation in the fabric of space-time described by a metric:

$$G_{\mu\nu} = k^2 T_{\mu\nu},$$

Where $G_{\mu\nu}$ is the Einstein tensor and $T_{\mu\nu}$ is the stress-energy tensor. k^2 is the **Einstein gravitational constant**, defined as:

$$k^2 = \frac{8\pi G}{c^4} \approx 2.07664744 \times 10^{-43} N^{-1}$$

Where G is the Newtonian constant of gravitation and c is the speed of light in vacuum. Thought the entire work we use $c \rightarrow 1$, so all the speeds are represented in fractions of this constant. This field equation describes how the curvature of space-time (LHS) changes based on the properties of energy-matter (RHS). Numerous models have been established since the first interior and exterior solutions were given by Einstein himself (1915) and Schwarzschild (1916) [4]. In subsequent years, Richard C. Tolman worked on spherically symmetric, static and perfect fluids driven by isotropic matter, providing new solutions in terms of previous explicit analytic functions[5].

A star is a plasma comprised object held together by self-gravity. The astronomical object formed by a high temperature fluid can be understood in terms of the gravitational field produced by itself; due to the large amount of relative mass and energy, it can wrap its own material into an spherically symmetric object with a energetic self-sustained system given by the nuclear reactions inside of it. [6]. The physicist's duty is studying the nature of this gravitational field in both interior and exterior regions.

1.1 Problem statement

Many fundamental solutions describing the structure of internal gravitational fields for stellar objects have been attained by solving exactly or numerically the Einstein field Equations (EFE); the so called, interior solutions are described as ideal static fluid spheres driven by isotropic matter given a spherically symmetric space-time. A large amount of isotropic solutions satisfy the physical acceptable conditions. Einstein (1915), Schwarzschild (1919) and Tolman (1939) proposed the first solutions to the EFE, unfortunately they had to input arbitrary conditions to solve easily the resultant system of differential equations. The models obtained in the solution of such ideal systems lead to state variables that describe a model of stellar objects, but that was not completely described in reality, due to the fact that many of the state properties, and components of them were sacrificed for simplicity.

In order to make them more realistic, there is a necessity of introducing non-isotropic parameters on the already given solutions, so we can develop a more reasonable model for stellar objects. The difficulty to handle the EFE conducted to new ways of solving these systems. One of these forms is called Minimal Geometric Transformation by gravitational decoupling; a technique that allows us to take a previous tested solution, and adopt it as seed material for the new resultant solution. The main problem on this approach is to find a seed solution physically acceptable that can grant a non-ideal solution, then test it, so we can find if the new solution is also physically acceptable [7].

1.2 Objectives

1.2.1 General Objective

The current monograph introduces a modern systematic form for solving the Einstein Field Equations in an exact way, by introducing the Minimal Geometric Deformation by Gravitational Decoupling used as a powerful tool to handle EFE. It uses solutions that already have been tested as physically acceptable, and transform them into a unique form introducing anisotropy in the process, also making isotropic and perfect fluid solutions more realistic. The anisotropy is reflected in the new components of the pressure, tangential and radial, thus changing the original density too into a new one, called effective density (to differentiate from the original one). Testing the solution to see if it fulfils the physical conditions, and is applicable to any stellar object. We intend to use a previous given solution (Andrade-Einstein) already tested as an acceptable physical model, so we can apply the mentioned method, and get the new solution which is analyzed in order to find out if this new result fulfils the conditions of physical acceptability, and if it so it becomes an applicable system for stellar objects.

1.2.2 Specific Objectives

1.- Review General Relativity with a short introduction to differential geometry. and explore the classical solutions of the Einstein Field Equations (EFE).

2.- Introduce the Gravitational Decoupling and Minimal Geometric Deformation (MGD)

as mathematical tools to solve effectively the EFE, insert anisotropy inside perfect fluid solutions and obtain new stellar models.

3.- Perform an exploratory analysis on graphs related to each one of the acceptability conditions (Section 3.2), thence we can verify if the new solution is physically admissible.

In section 2, subsection 4 we present the different solutions for a isotropic and static stellar fluids aiming to understand the seed solutions later used in calculations using the MGD technique.

In section 3, subsection 1 we present the modern technique for finding anisotropic solutions by means of the isotropic ones.

In section 3, subsection 2 we introduce the conditions being used to verify if the new solutions are physically acceptable.

In section 3, subsection 3 we propose a seed solution used to perform the MGD technique.

Chapter 2

General Relativity

In this chapter we introduce all the theoretical framework to go deep into the main method we used in this thesis. First, a little presentation of the essential root of the entire work: General Relativity, some concepts on differential geometry and the Einstein Field Equations (EFE) where we introduce the mathematical machinery necessary for developing the work. The final subsection presents the historical solutions to the EFE; we introduce Einstein, Schwarzschild and Tolman classical results.

2.1 General Relativity

It is well appreciated that gravity is a special type of fundamental interaction. The fact that the driving field that originates the gravitational "force" is the metric describing the four dimensional physical space, makes us wonder if we are dealing with a real force. Einstein developed the idea of a curved space-time and a metric due to the universality of gravity characterized by the Principle of Equivalence. It occurs in various forms, three main branches of this principle cover all aspects of gravitational fields, and their perceptions in a four dimensional space. The Weak Equivalence Principle (WEP) states that gravitational mass and inertial mass are equivalent, hence the name. $m_g = m_i$ [8]. The implications of this statement consider the fact that single particles in "free fall" are not sufficient to distinguish a uniformly accelerated reference frame from a gravitational field. However, we must be judicious with the tempting idea of considering impossible to distinguish gravity from an accelerated frame. In fact, the framework where that conception operates is a relative "small region of space". Therefore, we can reformulate the WEP

as follows: "the motion of free falling particles are the same in gravitational fields as in uniformly accelerated reference frames, in small enough regions of space" [9].

Special relativity (SR) taught us that mass is just another instance of the energy-momentum (4-vector p^μ). With the valid motive of generalizing the WEP statement into a new one including SR, he conceived the well known Einstein Equivalence Principle (EEP). It states "In sufficiently small regions of space, the laws of physics reduce to those of special relativity: it is impossible to detect the presence of a gravitational field by means of local experiments". This implies that there is no such thing as a "neutral object" from where we can measure acceleration due to gravity. So, it becomes clear that we can interpret "unaccelerated" as "free falling". The last branch is called Strong Equivalence Principle that includes the non-gravitational laws of physics, but we will work with the first two due to the fact that we are dealing only with gravitational stellar sources [9].

The concept of "small region" of a space is pretty ambiguous. If we want to construct some approach on flat or curved space-time, there is a mathematical concept called differential manifolds that can help us understand the vague idea of local flatness and global curved four dimensional space [1].

2.2 Manifolds in Differential Geometry

These are one of the most fundamental concepts in mathematics and physics. A pretty intuitive definition of a manifold is something that appears to be globally curved if we observe the entire mathematical object, but if we take a closer look into a single and "small region", it seems to be locally flat or that assumes the same properties as a Euclidean space. Formally speaking, the global picture can contain a complex topology, but the local sector can appear to be like R^n [9]. It is important to notice that in the limit where the space-time volume goes to zero, the twisted space becomes flat, so we can say that this space is created by summing this different infinitesimal sectors up to the global figure, "sewing" them in different directions.

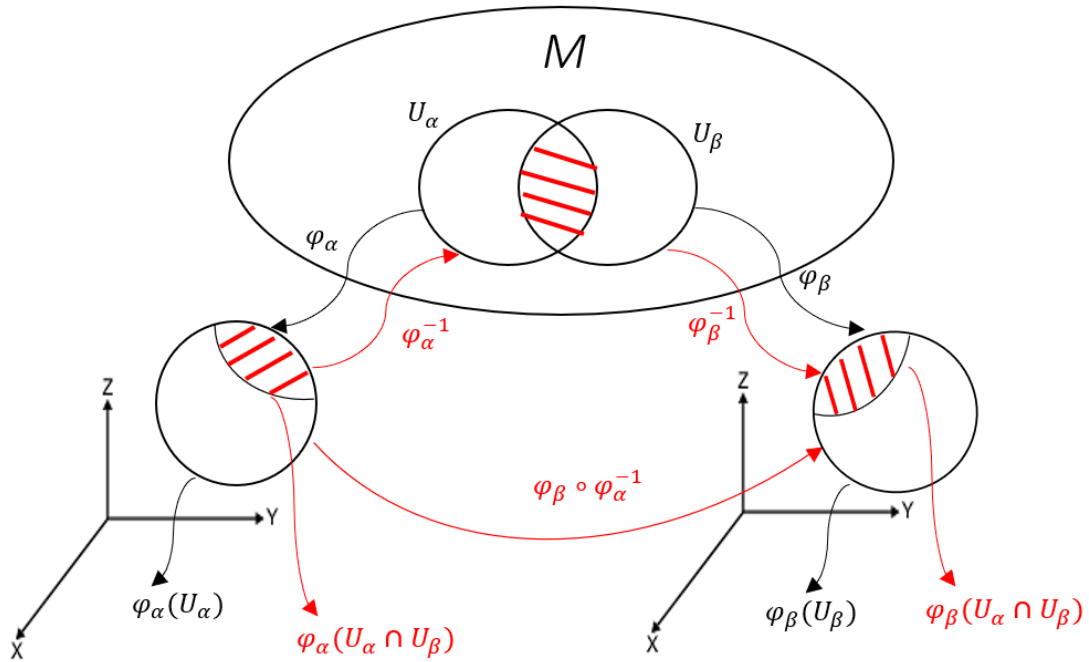


Figure 2.1: Mapping: $(M \rightarrow R^n)$ from Manifold to Euclidean Space

The precise mathematical definition of a manifold is the following: A manifold is a topological space with the property that each point has a neighborhood that is homeomorphic to an open subset of an n -dimensional Euclidean space [10]. One of the most important aspects of manifolds in physics is if it is differentiable or not, what we mean with that is that if it have a tangent space at each point that can be described with some kind of derivative (more general concept of differentiation of functions). A formal definition declares, a differentiable manifold is a topological manifold with a globally defined differential structure [10]. The smoothness is related with this property of manifolds; hence, it is important to notice if some described physical space does not have singularities. Furthermore, one critical notion from GR that relates deeply with manifolds, and it is the core for generating solutions of the Einstein Field Equations is the metric. The metric is a Tensor, whose components usually written as $g_{\mu\nu}$, are adopted to describe certain curved space, while inverse components are usually written $g^{\mu\nu}$. In physics, it allows us to characterize certain properties of space time, we can list the following [9]:

- The notion of past and future.
- The calculations of path length and proper time, also the Geodesic for particle's

motion.

- A Metric replacing Newtonian gravitational classical field, so gravity is just a consequence of having space described by a certain geometry.
- The definition of locally inertial frame.
- The information about causality on events contained in the metric.
- The reformulation of the line element approach as follows:

$$ds^2 = g_{\mu\nu}^2 dx^\mu dx^\nu. \quad (2.1)$$

- The Line elements that can help us calculate the length of curves, given by:

$$\int_{\partial S} |g_{\mu\nu} \frac{dx^\mu}{d\lambda} \frac{dx^\nu}{d\lambda}|^{1/2} d\lambda. \quad (2.2)$$

- The tool (Metric) to raise or lower tensorial components:

$$V_\alpha = g_{\alpha\beta} V^\beta. \quad (2.3)$$

Some other important aspects of a metric can be referred to its canonical form and signature. In this form, the components of the metric tensor can become:

$$M = \text{diag}(-1, -1, -1, \dots, +1, +1, +1, \dots, 0, 0, 0). \quad (2.4)$$

With *diag* correspondent to diagonal matrix; the signature refers to the sum of the signs from the main diagonal of the metric, usually +2 or -2 for GR. It is worth say that the eigenvalues define the positiveness of a metric, they can be positive, negative or zero (degenerate), so the signatures determine the positiveness. With this concept in mind, we can define the mathematical foundation of GR inside differential geometry [1].

2.2.1 Riemannian and pseudo-Riemannian Manifolds

A Riemannian manifold, after the mathematician Bernard Riemann, is a real differential manifold M that has the property of positive-definiteness on its inner product g_p on a

target space T_p at each point p . This means, all of its eigenvalues are positive. This mathematical object can be defined with a manifold M and a metric $g(M, g)$, so the geometric properties of this space such as distance, angles at intersections, length, area and also curvature of the manifold are completely described by the metric [11]. We can derive a broader notion of Riemannian manifolds, based on the fact that some of the eigenvalues can also be negative. This is called a pseudo-Riemannian manifold; it helps us understand completely the geometric notions of General Relativity. The wide spectrum of eigenvalues, that are non-degenerate (non zero), gives the indefinite property on the inner product.

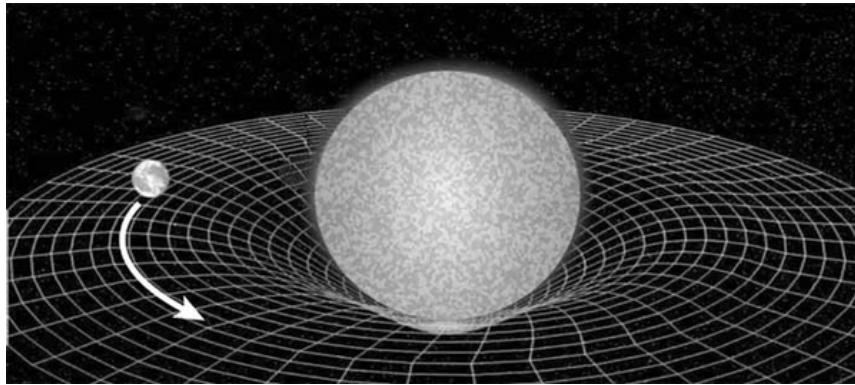


Figure 2.2: Curved space-time due to the presence of mass-energy (stellar object). Image source: https://uh.edu/~jclarage/astr3131/lectures/4/einstein/Einstein_stanford_Page7.html

2.3 Einstein Field Equations (EFE)

Previously, we dealt with the mathematical background of GR. Henceforth, we introduce the analytical engine that allows us to manipulate and solve the EFE. Tensor calculus and differential geometry, are the tools we require to reconstruct these equations and find different solutions. Forthwith, we analyze the intuition behind the central components of the EFE, and show how to deduce the final form of the system in terms of the previous numerical calculations. Moreover, this section is intended to detail the physical meaning of each tensorial factor that integrates the EFE.

2.3.1 The Riemann Tensor and Curvature

One of the most important characteristics of Riemann Tensor is the calculation of the curvature at each point for a given region of space (geometry). The way we describe a curved space is by means of a metric tensor. Given a locality in space-time, we calculate the components of a tensor following the direction of the geodesic (a curve minimizing the local path length of certain space) [1]. Vector components remain constant when parallel transport occurs in a closed loop.

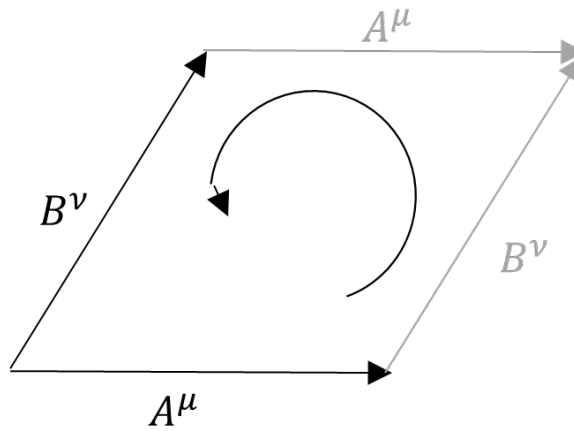


Figure 2.3: Parallel Transport of a first-rank tensor around a closed loop

The Riemann tensor describes the local curvature at each point inside this 'small region' of space. We can imagine two infinitesimal displacement vectors A^μ and B^ν , and a random vector in that space V^σ . We can imagine the parallel transport of the V^σ vector in the closed formed by A^μ and B^ν vectors (Fig. 2.3). For instance, we can start in A^μ , then go along B^ν , then backwards in direction of A^μ , and finally in the opposite direction of B^ν , so that way we can create an infinitesimal closed loop [9]. Forthwith, we want to know if there is a change in the components of the V vector when parallel transported around the closed circuit (A^μ, B^ν) (Fig. 2.3). Therefore, we can calculate the infinitesimal change δV^ρ as follows:

$$\delta V^\rho = R^\rho_{\sigma\mu\nu} V^\sigma A^\mu B^\nu. \quad (2.5)$$

In Eq. (2.5), we introduce a new tensorial factor. This term is the Riemann tensor, and it is a fourth-rank tensor responsible for calculating the local curvature on each point,

so we can figure out directly the infinitesimal change in vector V^σ around the given loop. The calculation of this tensor is made in relation with the "connection coefficients" or "Christoffel symbols" (Γ_{jk}^i) [12].

The Christoffel symbols are the representation of components of a non tensorial element, a mathematical tool that helps us relate the covariant derivatives of metric components in one coordinate system to another. Also, it helps determining the Levi-Civita connection. In that way, we can find the components of Riemann tensor [13]:

$$R_{\sigma\mu\nu}^\rho = \partial_\mu \Gamma_{\nu\sigma}^\rho - \partial_\nu \Gamma_{\mu\sigma}^\rho + \Gamma_{\mu\lambda}^\rho \Gamma_{\nu\sigma}^\lambda - \Gamma_{\nu\lambda}^\rho \Gamma_{\mu\sigma}^\lambda. \quad (2.6)$$

It is possible to find the all the Christoffel coefficients (considering it is not a tensor) related to the unique connection, when this is **metric compatible** and **torsion free** [9]:

$$\Gamma_{\mu\nu}^\sigma = \frac{1}{2} g^{\sigma\rho} (\partial_\mu g_{\nu\rho} + \partial_\nu g_{\rho\mu} - \partial_\rho g_{\mu\nu}). \quad (2.7)$$

As mentioned before, the components of the Riemann tensor helps us find the curvature for each point in a space with certain metric; it is important to notice that if the Riemann tensor vanishes Eq. (2.8), then the metric represents a flat space, and if not, there is a curvature associated [9].

$$R_{\sigma\mu\nu}^\rho = 0 \text{ (Flat Space)}. \quad (2.8)$$

A remarkable property is the fact it has only one contraction, the so-called Ricci Tensor ($R_{\alpha\beta}$), it is a symmetric second rank tensor and fundamental element in defining EFE[1]:

$$R_{\alpha\beta} = R_{\alpha\mu\beta}^\mu = R_{\beta\alpha}. \quad (2.9)$$

Similarly, it is possible to define the Ricci Scalar R by means of the metric tensor $g^{\mu\nu}$ in its contravariant form, and the Ricci tensor defined in Eq. (2.9):

$$R = g^{\mu\nu} R_{\mu\nu} \quad (2.10)$$

We are going to use these tools in following sections.

2.3.2 Energy-Stress Tensor and Fluid Motion

Before going deep into the derivation of EFE, we depict the tensorial form of energy-matter sources. Essentially, the presence of energy-matter source originates the curvature of space time. The stress-energy tensor defines the properties of the source we are dealing with, and detail the density and flux of energy and momentum in space time [14]. In this case, the perfect fluid energy-stress tensor introduces an effective modeling tool for astronomical bodies, such as stars or the Universe itself.

In order to calculate this tensor, we start defining the fundamental properties for a relativistic ideal fluid. To begin with, we can represent the motion of a particle with its 4-momentum p^μ given by:

$$p^\mu = mu^\mu = \gamma mv^\mu = (\gamma mc, \gamma m\mathbf{v}) = (E/c, \mathbf{p}). \quad (2.11)$$

Directly, we pass to a continuous distribution of matter such as fluids in motion. A perfect fluid is characterized by two scalar fields: ρ defining the density and p describing its pressure, also a 4-velocity field u^μ is required to construct the motion of the particles. In exchange of the 4-momentum $p^\mu = mu^\mu$, we have the 4-momentum density ρu^μ . In addition, we need to specify a certain metric $g^{\mu\nu}$. Fundamentally, we can describe a fluid source with a second rank tensor $T^{\mu\nu}$. This tensor needs to fulfil the conservation of energy given by the following equation [15]:

$$\nabla_\mu T^{\mu\nu} = 0. \quad (2.12)$$

It is important to remark that the conservation equation Eq. (2.12) works for all fluids and all sources, not just the ideal one. Now, putting all these properties into consideration, we have the general formula for the tensor components describing the ideal fluid:

$$T^{\mu\nu} = (\rho + p/c^2)u^\mu u^\nu - pg^{\mu\nu}. \quad (2.13)$$

Firstly, we can notice that this tensor is symmetric:

$$T^{\mu\nu} = T^{\nu\mu}. \quad (2.14)$$

Also, if we set the conservation equation Eq. (2.12) for $T^{\mu\nu}$, and then expand the expression. We can find two classic equations, the continuity equation and Euler's equation of motion for perfect fluid dynamics (adiabatic and zero-viscosity flow) [12]. We fix them in vector form:

$$\frac{\partial \rho}{\partial t} + \nabla \cdot (\rho \mathbf{v}) = 0 \quad (\text{Continuity Equation}), \quad (2.15)$$

$$\rho \left(\frac{\partial}{\partial t} + \mathbf{v} \cdot \nabla \right) \mathbf{v} = -\nabla p \quad (\text{Euler's Equation}). \quad (2.16)$$

Ideal gases or poly-tropic fluids are commonly used to describe stellar material. In summary, The perfect fluid concept in GR is given by a fluid completely described just by its mass-density ρ and isotropic pressure p ; it has zero viscosity, zero thermal conduction, and null shear stress.

2.3.3 The Field Equations from Riemann Geometry

Now, we are ready to derive the EFE. Starting with the Newtonian field equations given by the Poisson's equation:

$$\nabla^2 \phi = 4\pi G \rho. \quad (2.17)$$

We can generalize Eq. (2.17) by considering an equation relating space and source, in one side the operator defining the curvature of space, and in the opposite side an operator defining the energy source. Describing as follows:

$$\mathbf{O}(g^{\mu\nu}) = k^2 \mathbf{T}. \quad (2.18)$$

The operator \mathbf{O} depends on a metric. The expansion of Eq. (2.18) in terms of the tensor components is given by:

$$O^{\mu\nu} = R^{\mu\nu} + \alpha R g^{\mu\nu}. \quad (2.19)$$

Where α is an unknown constant describing the fraction of geometric inertia of the given space. Notice that these calculations were made considering the contra-variant form of the tensors, but they work the same way with the covariant formulation. Just multiply

by the covariant metric $g_{\mu\nu}$ to transform the components.

The Einstein equivalence principle states that the conservation of energy-momentum is required.

$$\nabla_{\mu} O^{\mu\nu} = \nabla_{\mu} T^{\mu\nu} = 0, \quad (2.20)$$

$$\nabla_{\mu} O^{\mu\nu} = \nabla_{\mu} (R^{\mu\nu} + \alpha R g^{\mu\nu}) = 0. \quad (2.21)$$

We use the Bianchi identities to identify the missing constant α , so we find that the only value that makes it zero when applied the divergence operator is $\alpha = -\frac{1}{2}$. This completes $O^{\mu\nu}$ operator, and the entire expression is called the Einstein tensor denoted as $G^{\mu\nu}$ [1].

$$G^{\mu\nu} = R^{\mu\nu} - \frac{1}{2} R g^{\mu\nu}. \quad (2.22)$$

Now, we have completed the EFE, represented in tensorial form, relating the Einstein curvature tensor and the energy-stress tensor, resulting in:

$$G^{\mu\nu} = R^{\mu\nu} - \frac{1}{2} R g^{\mu\nu} = k^2 T^{\mu\nu}. \quad (2.23)$$

2.4 Fundamental Solutions

Here, we acquaint with the traditional and early solutions for Einstein Field Equations. Three main solutions are taken for analysis: the Einstein Solution for a static universe, the Schwarzschild-de Sitter solution for vacuum, and the Tolman IV solution. These results were proposed as seeds for the modern method (MGD) of working out the EFE, thus access new non-isotropic outcomes. In 1939, Richard Tolman submitted a paper of solutions for EFE, considering the matter sector as perfect fluid, and a general metric describing a spherically symmetric curved space-time, we can see these terms along these lines [5].

The energy-stress tensor describing the perfect fluid Eq.(2.13):

$$T_{\mu\nu}^{(m)} = (\rho + p)u_{\mu}u_{\nu} - pg_{\mu\nu}, \quad (2.24)$$

$$T = \begin{bmatrix} \rho & 0 & 0 & 0 \\ 0 & -p & 0 & 0 \\ 0 & 0 & -p & 0 \\ 0 & 0 & 0 & -p \end{bmatrix}.$$

The line element \mathbf{ds} derived using the spherically symmetric general form of metric tensor \mathbf{g} :

$$ds^2 = e^{\nu(r)} dt^2 - e^{\lambda(r)} dr^2 - r^2(d\theta^2 + \sin^2 \theta d\phi^2). \quad (2.25)$$

Also we have the matrix correspondent to the metric tensor:

$$(g_{\mu\nu}) = \begin{bmatrix} e^{\nu(r)} & 0 & 0 & 0 \\ 0 & -e^{\lambda(r)} & 0 & 0 \\ 0 & 0 & -r^2 & 0 \\ 0 & 0 & 0 & -r^2 \sin^2 \theta \end{bmatrix}.$$

It is important to notice that metric components usually come in the form of a line element, relating the metric entries with the coordinates differentials used to describe the space-time. In this case, it is simple to observe that Tolman (1939) used spherical coordinates to derive easier to solve equations.

Using EFE, the energy-stress tensor and the metric components, we can retrieve a system of differential equations with 4 unknowns but just 3 equations.

$$-k^2 \rho = -\frac{1}{r^2} + e^{-\lambda} \left(\frac{1}{r^2} - \frac{\lambda'}{r} \right), \quad (2.26)$$

$$k^2 p = -\frac{1}{r^2} + e^{-\lambda} \left(\frac{1}{r^2} + \frac{\nu'}{r} \right), \quad (2.27)$$

$$k^2 p = \frac{e^{-\lambda}}{4} \left(2\nu'' + \nu'^2 - \lambda'\nu' + 2\frac{\nu' - \lambda'}{r} \right). \quad (2.28)$$

Tolman (1939) reformulated the Eq. (2.28), so it can be affordable to solve:

$$\frac{d}{dr} \left(\frac{e^{-\lambda} - 1}{r^2} \right) + \frac{d}{dr} \left(\frac{e^{-\lambda} \nu'}{2r} \right) + e^{-\lambda-\nu} \frac{d}{dr} \left(\frac{e^{\nu} \nu'}{2r} \right) = 0. \quad (2.29)$$

It was fundamental to introduce some arbitrary constraint, so we can add another equation to the set, and make it a complete 4x4 system of differential equations. In case of the main three solutions, 3 different restrictions were given by their correspondent authors [16, 4, 5]. Thus, we can follow the main results. New constants of integration will be introduced in the outcomes (A,B,R,m,c) [5].

2.4.1 Einstein Static Universe Solution

Restriction:

$$e^{\nu} = \text{constant}, \quad (2.30)$$

Results

$$e^{\lambda} = \frac{1}{1 - \frac{r^2}{R^2}}, \quad (2.31)$$

$$e^{\nu} = c^2, \quad (2.32)$$

$$k^2 \rho = \frac{3}{R^2}, \quad (2.33)$$

$$k^2 p = -\frac{1}{R^2}. \quad (2.34)$$

R, c are constants of integration

2.4.2 Schwarzschild-de-Sitter Solution

Restriction:

$$e^{-\lambda-\nu} = \text{constant}. \quad (2.35)$$

Results

$$e^\lambda = \left(1 - \frac{2m}{r} - \frac{r^2}{R^2}\right)^{-1}, \quad (2.36)$$

$$e^\nu = c^2 \left(1 - \frac{2m}{r} - \frac{r^2}{R^2}\right), \quad (2.37)$$

$$k^2 \rho = \frac{3}{R^2}, \quad (2.38)$$

$$k^2 p = -\frac{3}{R^2}. \quad (2.39)$$

R, c, m are constants of integration.

If we take $R \rightarrow \infty$, we get the primal Schwarzschild solution for vacuum, and the correspondent metric line element represented as:

$$ds^2 = c^2 \left(1 - \frac{2m}{r}\right) dt^2 - \left(1 - \frac{2m}{r}\right)^{-1} dr^2 - r^2 (d\theta^2 + \sin^2\theta d\phi^2). \quad (2.40)$$

2.4.3 Tolman IV Solution

Restriction:

$$\frac{e^\nu \nu'}{2r} = \text{constant}. \quad (2.41)$$

Results

$$e^{\nu(r)} = B^2 \left(1 + \frac{r^2}{A^2}\right), \quad (2.42)$$

$$e^{-\lambda} = \frac{(1 - \frac{r^2}{C^2})(1 + \frac{r^2}{A^2})}{1 + \frac{2r^2}{A^2}}, \quad (2.43)$$

$$k^2 \rho(r) = \frac{3A^4 + A^2(3c^2 + 7r^2) + 2r^2(c^2 + 3r^2)}{c^2(A^2 + 2r^2)^2}, \quad (2.44)$$

$$k^2 p(r) = \frac{c^2 - A^2 - 3r^2}{c^2(A^2 + 2r^2)}. \quad (2.45)$$

A, B, R, c are constants of integration.

It is fundamental to emphasize, that these solutions were postulated on the assumption that we have an ideal mass-energy object, like a perfect fluid, and also we have a spherically symmetric space-time. In reality, we have non-isotropic and pseudo-spherical symmetric stellar object [17]. The main issue relapses on the fact that even if they are "good" models,

they do not describe an stellar object with great precision; consequently, we need some kind of approach that enables us to introduce anisotropy (non-perfect behavior) into these models, we describe this terms in next section.

Chapter 3

Methodology

3.1 Minimal Geometric Deformation by Gravitational Decoupling

In this section we present the essentials of the Minimal Geometric Deformation (MGD) technique that allows us to get a new solution based on a seed one. Subsequently, we define certain conditions for a solution to be considered a real physical model, where we can develop the physics inside the problem. Finally, the Andrade-Einstein solution for an isotropic universe is used as the central seed for finding a new solution.

The MGD method appears as an important extension of the GR world into a subject more general that we can apply in order to find new models and solutions to the EFE. We can also study gravity in higher dimensions; and the most important part is that we can obtain the equations of GR by just taking certain parameters out of equation, so we can say it is a good generalization. One of the simplest ways of generalizing the ideas behind GR is to take the Einstein-Hilbert action and to add another term into the integral [18]:

$$S = \int \left(\frac{R}{2k^2} + \mathcal{L}_M \right) \sqrt{-g} dx^4 + \alpha(\text{correction}). \quad (3.1)$$

Where α is a control parameter used to introduce the new correction or deformation, but if we want to retrieve the equations of GR we can just set $\alpha = 0$. So we know that the idea of deformation is just an extension, and not the development of another branch.

$$\text{Geometric Deformation} = X + \alpha Y. \quad (3.2)$$

The MGD method by gravitational decoupling was originally proposed in the context of the Randall–Sundrum brane-world [18] and extended to investigate new black hole solutions [19, 20]. It is a modern technique we can use as a tool to extend solutions of a spherically symmetric space-time and perfect fluid solutions into a more general one. We can add certain parameters into the equations, so we can adjust the structure of the equations, but without changing its essence, so they continue to be EFE.

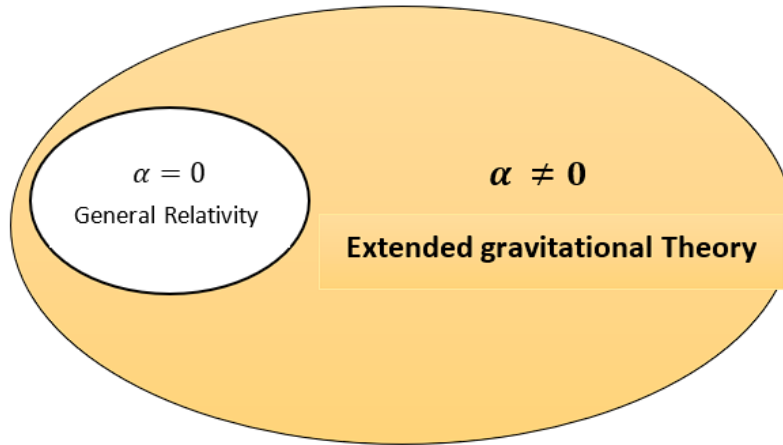


Figure 3.1: MGD as an extension of General Relativity.

The important aspects of MGD start with a simple source or "seed", which is an original solution that we can extend by adding another term. It is as simple as taking the energy-stress tensor and sum another tensor. This tensor represents an extra gravitational source that will change the ideal behavior of the perfect fluid (deformation tensor), but with an extra parameter (for previous work on MGD see [21, 22]).

$$\hat{T}_{\mu\nu} \mapsto \hat{T}_{\mu\nu}^{(1)} = \hat{T}_{\mu\nu} + \alpha^{(1)}\hat{T}_{\mu\nu}^{(1)}. \quad (3.3)$$

The method allows us to extend the solutions as much as we want, even if we just use as the seed the previous extended result over and over again.

$$\hat{T}_{\mu\nu}^{(1)} \mapsto \hat{T}_{\mu\nu}^{(2)} = \hat{T}_{\mu\nu} + \alpha^{(2)}\hat{T}_{\mu\nu}^{(2)}. \quad (3.4)$$

As shown in the previous section, the stress-energy tensor has to fulfil the conservation of energy condition:

$$\nabla_{\nu} \hat{T}^{\mu\nu} = 0. \quad (3.5)$$

Before dealing with the EFE, we have to introduce a certain tensor $\theta_{\mu\nu}$ describing an external deformation source. This is included with an α constant adding up to the original source, in this case a tensor describing a perfect fluid. Then, the total stress-energy tensor is written as:

$$T_{\mu\nu}^{(Tot)} = T_{\mu\nu}^{(m)} + \alpha\theta_{\mu\nu}. \quad (3.6)$$

The method stands for splitting the resultant system of equations into two systems that are easily solvable, we can observe in Eq. (3.6) that the system can be divided into the original field equations and the pseudo system containing the components of deformation tensor [7]. It is important to remind that all the sources have to fulfil the energy-momentum conservation equation, it does not matter how many deformations we include in total (Tot).

$$\nabla_{\nu} T^{(Tot)\mu\nu} = 0. \quad (3.7)$$

In summary, the method relies on introducing a deformation $\theta_{\mu\nu}$, and then after doing some algebra decouple the original EFE into two systems of equations, A and B. The standard EFE are solved for A, and a much more simple system, called quasi-Einstein Field Equations are solved for B. We then, sum up the solutions including the α factor to identify the original solution and the deformation. After that, we have the new solution given by $A \cap B$ [7].

Due to the fact that, EFE are a non-linear set of equations, the method described above represents an advanced technique to introduce new solutions into the large amount of perfect fluid solutions already given along the more than hundred years of investigation [23]. It is crucial to emphasize, that the decoupling of the system works due to the spherical symmetry of the metric, and the independence on time t for each component of the metric. They just depend on the radius r .

There are multiple already-described systems that we can mention right now, as relevant examples given by Ovalle(2018) on the applicability of this approach, such us Einstein-Maxwell [24], Einstein-Klein-Gordon system [25, 26], for higher derivative gravity [27], f

(R)-theories of gravity [28, 29].

3.1.1 Gravitational Decoupling of Einstein Field Equations

The method starts with traditional EFE including the deformation (in this case we include a minus sign in front of k^2 constant, so we have easier calculations later):

$$R_{\mu\nu} - \frac{1}{2}Rg_{\mu\nu} = -k^2T_{\mu\nu}^{(Tot)}. \quad (3.8)$$

The original source is described by the perfect fluid Eq. (2.24). In case of asking for the missing light speed constant c , we address the problem by considering the major constants of the equations as equal to one. The velocities are considered as fraction of light speed $\frac{v}{c}$.

$$T_{\mu\nu} = T_{\mu\nu}^{(m)} = (\rho + p)u_\mu u_\nu - pg_{\mu\nu}. \quad (3.9)$$

We then introduce the spherically symmetric metric for EFE as follows:

$$ds^2 = e^{\nu(r)}dt^2 - e^{\lambda(r)}dr^2 - r^2(d\theta^2 + \sin^2\theta d\phi^2). \quad (3.10)$$

Substituting Eq. (3.6) in Eq. (3.8), we get the new field equations in terms of the new total energy tensor components. These can be treated as an anisotropic fluid [30]. Notice we have not decoupled the equations yet. Also, consider the fact we expressed the θ components in terms of its tensor mixed form (one index down and one up) Eq. (3.11-3.13), due to the fact that this form shows implicit multiplication of the original covariant components $\theta_{\mu\sigma}$ with the contra-variant form of the metric $g^{\sigma\nu}$. This is just algebraic manipulation, so we can set the equations in their less complicated expression.

$$-k^2(\rho + \alpha\theta_0^0) = -\frac{1}{r^2} + e^{-\lambda} \left(\frac{1}{r^2} - \frac{\lambda'}{r} \right), \quad (3.11)$$

$$-k^2(-p + \alpha\theta_1^1) = -\frac{1}{r^2} + e^{-\lambda} \left(\frac{1}{r^2} + \frac{\nu'}{r} \right), \quad (3.12)$$

$$-k^2(-p + \alpha\theta_2^2) = \frac{e^{-\lambda}}{4} \left(2\nu'' + \nu'^2 - \lambda'\nu' + 2\frac{\nu' - \lambda'}{r} \right). \quad (3.13)$$

As a reminder, the total stress-energy tensor fulfils the conservation equation, and can

be expanded in terms of the original and new deformation components:

$$p' + \frac{\nu'}{2}(\rho + p) - \alpha(\theta_1') + \frac{\nu'}{2}\alpha(\theta_0^0 - \theta_1^1) + \frac{2\alpha}{r}\alpha(\theta_2^2 - \theta_1^1) = 0. \quad (3.14)$$

The new variables observed in the left side of system Eq. (3.11-3.11) indicate changes in the state functions of the object due to the introduction of the deformation components. The $\tilde{\rho}$ represents the effective density Eq. (3.11). Now there are two components for the pressure, the radial component $\tilde{p}_r = \rho - \alpha\theta_1^1$ Eq. (3.12) and the tangential component $\tilde{p}_t = \rho - \alpha\theta_2^2$ Eq. (3.13).

$$\tilde{\rho} = \rho + \alpha\theta_0^0, \quad (3.15)$$

$$\tilde{p}_r = p - \alpha\theta_1^1, \quad (3.16)$$

$$\tilde{p}_t = p - \alpha\theta_2^2. \quad (3.17)$$

Notice, in this case pressure is not isotropic anymore, it has components, and that expresses an important goal of this work, the introduction of anisotropy inside an ideal system. We can describe anisotropy by the following formula:

$$\Gamma = \tilde{p}_t - \tilde{p}_r = \alpha(\theta_1^1 - \theta_2^2). \quad (3.18)$$

In order to implement the MGD approach, we can start by changing the general form of the metric Eq. (3.10) into the following:

$$ds^2 = e^{\xi(r)} dt^2 - \frac{dr^2}{\mu(r)} - r^2(d\theta^2 + \sin^2\theta d\theta^2). \quad (3.19)$$

From here, the standard new form of radial component $\mu(r)$ can be calculated in terms of the mass:

$$\mu(r) = 1 - \frac{k^2}{r} \int_0^r x^2 \rho dx = 1 - \frac{2m(r)}{r}. \quad (3.20)$$

Straightaway, the MGD approach introduces a change in terms of new unknown functions $f(r)$ and $g(r)$ in the radial and temporal elements of the metric Eq. (3.10). The deformation is not only implemented inside the stress-energy tensor, but in the general

metric as well. The same parameter α is used as the degree of the deformation. It can take values inside the interval $[0, 1]$ (that is why the name Minimal).

$$\xi \mapsto \nu = \xi + \alpha g, \quad (3.21)$$

$$\mu \mapsto e^{-\lambda} = \mu + \alpha f. \quad (3.22)$$

The simplest way of performing the MGD sets the temporal deformation Eq. (3.21) equals zero and lets the spatial change Eq. (3.22) untouched, that is the easiest way of decoupling the system of equations Eq. (3.11-3.13), so only the spatial element becomes deformed:

$$g \mapsto 0, \quad (3.23)$$

$$f \mapsto f^*. \quad (3.24)$$

It is easy to calculate the change in $\mu(r)$ parameter with the introduction of the new variable f :

$$\mu(r) \mapsto e^{-\lambda(r)} = \mu(r) + \alpha f^*(r). \quad (3.25)$$

Upon replacing the Eq. (3.22) into the system Eq. (3.11-3.13), we can perform the decoupling just by observing the variables which are preceded by α and the ones that are not. The resultant system is divided into two systems, the original EFE containing the seed solution, and the new quasi-Einstein Field Equations that helps us find the components of the deformation θ .

The original system reads:

$$k^2 \rho = \frac{1}{r^2} - \frac{\mu}{r^2} - \frac{\mu'}{r}, \quad (3.26)$$

$$k^2 p = -\frac{1}{r^2} + \mu \left(\frac{1}{\nu} + \frac{\nu'}{r} \right), \quad (3.27)$$

$$k^2 p = \frac{1}{r^2} - \frac{\mu}{r^2} - \frac{\mu'}{r}. \quad (3.28)$$

The entire system fulfils the conservation equation condition, but it becomes splitted in

the same way as the system due to the linearity of the operator ∇_μ , and the introduction of the deformation as a linear sum.

$$\nabla_\mu(T^{\mu\nu} + \alpha\theta^{\mu\nu}) = 0. \quad (3.29)$$

Thus, for the system Eq. (3.26-3.28) the expanded conservation equation results.

$$p' + \frac{\nu'}{2}(\rho + p) = 0. \quad (3.30)$$

The quasi-system is:

$$k^2\theta_0^0 = -\frac{f^*}{r^2} - \frac{f^{*'}}{r}, \quad (3.31)$$

$$k^2\theta_1^1 = -f^* \left(\frac{1}{r^2} - \frac{\nu'}{r} \right), \quad (3.32)$$

$$k^2\theta_2^2 = -f^* \left(2\nu'' + \nu'^2 + 2\frac{\nu'}{r} \right) - \frac{\nu'}{r} \left(\nu' + \frac{2}{r} \right). \quad (3.33)$$

Now, the expanded conservation equation of this system Eqs. (3.31-3.33).

$$(\theta_1^1)' - \frac{\nu'}{2}(\theta_0^0 - \theta_1^1) - \frac{2}{r}(\theta_2^2 - \theta_1^1) = 0. \quad (3.34)$$

We can take a new metric out of the quasi-system Eq. (3.31-3.33).

$$ds^2 = e^{\nu(r)} dt^2 - \frac{dr^2}{f^*(r)} - r^2(d\theta^2 + \sin^2\theta d\theta^2). \quad (3.35)$$

It is important to consider the fact the quasi-system is not a complete EFE system. The system Eq. (3.31-3.33) is missing some terms to be complete, we can add those terms; that is why they are called pseudo EFE, but that does not affect the calculations of θ components.

$$\tilde{\rho} = \theta_0^0 + \frac{1}{k^2 r^2}, \quad (3.36)$$

$$\tilde{p}_r = \theta_1^1 + \frac{1}{k^2 r^2}, \quad (3.37)$$

$$\tilde{p}_t = \theta_2^2 = \theta_3^3. \quad (3.38)$$

A very crucial step into this method is recognizing that we can apply the approach

as many times as we want with multiple deformations $T_{\mu\nu}^{(i)}$ summed up to the provided seed solution without losing the original one due to the fact that the method of "minimal deformation" linearize the system Eq. (3.36-3.38). So, we can extend the technique as much as we can, but we have to contemplate the complexity of doing that multiple times.

$$T_{\mu\nu} = \tilde{T}_{\mu\nu} + \sum_{i=1}^n \alpha_i T_{\mu\nu}^{(i)}. \quad (3.39)$$

The system is not completely solved yet, we need specific conditions to fulfil, and certain constraints to complete the system.

3.1.2 External Metric and Matching Conditions

When we are dealing with differential equations we get functions with some unknown constants involved. We want to find out what the values of these constants are, and how they are related to each other; we need to consider initial and boundary conditions. The initial conditions are analyzed later. Here, in this case we are interested in the boundary conditions or so-called matching conditions.

Implementing the MGD technique helps us find the interior solution of a self-gravitating stellar object; just because of its own mass-energy composition. However, in real life we have external interference on the internal geometry due to the presence of other objects or external geometries [31], or even if we say that there is nothing around interfering. The matching conditions guide us into finding the unknown constants by means of equating both metrics at the boundary of the system, which in the case of stellar objects is their surface ($r = R$). We denote the elements (functions) of the interior metric ($r < R$) with a minus sign, and the external metric with a plus sign ($r > R$).

The interior metric can be written as:

$$ds^2 = e^{\nu^-(r)} dt^2 - \left(1 - \frac{2\tilde{m}(r)}{r}\right)^{-1} dr^2 - r^2(d\theta^2 + \sin^2\theta d\phi^2). \quad (3.40)$$

Where the $\tilde{m}(r)$ is called the interior mass function, and it can be related to the original mass with this formula.

$$\tilde{m}(r) = m(r) - \frac{r}{2}f^*(r). \quad (3.41)$$

The exterior metric is written as:

$$ds^2 = e^{\nu^+(r)}dt^2 - e^{\lambda^+(r)}dr^2 - r^2(d\theta^2 + \sin^2\theta d\phi^2). \quad (3.42)$$

Now, in the limit ($r = R$) the temporal, radial and other components of both metrics Eq. (3.40) and Eq. (3.42) have to match up. First, the temporal functions.

$$\nu^-(R) = \nu^+(R). \quad (3.43)$$

Then, the radial components.

$$1 - \frac{2M_o}{R} + \alpha f_R^* = e^{-\lambda^+(R)}. \quad (3.44)$$

We do not have to worry about the other components, since they have the same form in both metrics. Directly, the last form of the matching conditions handles the fact that at $r = R$ the radial internal pressure equates the pressure exerted by the external deformation. This is important, otherwise the stellar object would not be in hydrostatic equilibrium, and it would collapse. However, we cannot set the pressure directly to zero, this is just a special case.

The general statement for the pressure equilibrium at $r = R$ is given by

$$p(R) - \alpha(\theta_1^{1-}(R)) = -\alpha(\theta_1^{1+}(R)). \quad (3.45)$$

In most cases, the preferred external metric is the classic Schwarzschild metric, as a result of its low complexity to work with. This is a very special case because there is no external pressure or density outside the stellar object (vacuum external solution), and we can easily set the internal radial pressure equals to zero.

$$p_r(R) = 0. \quad (3.46)$$

Equations (3.43), (3.44) and (3.45) are the necessary and sufficient conditions for the

matching conditions, and a useful tool to find relations between constants.

3.1.3 Complete System of Equations: The Constrains

One big problem about the decoupled system of equations is the number of equations and variables. They do not match in numbers, we have 6 differential equations Eq. (3.26-3.28) and Eq. (3.31-3.33), but 7 unknowns (θ_0^0 , θ_1^1 , θ_2^2 , p_r , p_t , ρ , $f(r)$), so we need another extra equation, called constrain, in order to match up the numbers [7].

There are several ways to establish a constraint: we can use an equation of state, relating the state variables of the solution (p , ρ) [32]. Another way is implementing a complexity factor calculated by integration [33]. However, two commonly used constrains are called "mimic constrains", these are the ones we are going to adopt in this work because they make the system of equations easier to solve.

The mimic constrains set the temporal and radial deformation elements equal to the seed density and pressure correspondingly. It is important to mention that these conditions are arbitrary, and we can give another equation relating the state variables of the stellar object, for instance an state equation.

Mimic Constraint for the Pressure:

$$\theta_1^1(r) = p(r). \quad (3.47)$$

Mimic Constraint for the Density:

$$\theta_0^0(r) = \rho(r). \quad (3.48)$$

Once we have completed the system of equations with the constraints Eq. (3.47) or Eq. (3.48), we can solve it. Given the variables of the seed solution, if isotropic ($p(r)$, $\rho(r)$, $\nu(r)$, $\mu(r)$), we apply the mimic constraints one or another to find the anisotropic solution for the original system.

We can start by analyzing the mimic constraint for the pressure.

$$k^2 p(r) = -f^* \left(\frac{1}{r^2} - \frac{\nu'}{r} \right). \quad (3.49)$$

Take the original system Eq. (3.26-3.28), and solve for pressure $p(r)$, we replace this equation into Eq. (3.27) to find $f(r)$.

$$f^*(r) = -\mu(r) + \frac{1}{1 + r\nu'(r)}. \quad (3.50)$$

The mimic constraint for density leads us to a first order differential equation, when we introduce the constraint into Eq. (3.26), rearrange it, and solve it for $f(r)$

$$f'(r) + \frac{f(r)}{r} = -rk^2\rho(r). \quad (3.51)$$

Once we have found $f(r)$ with Eq. (3.50), we can calculate the temporal $\nu(r)$ and radial $\mu(r)$ components of the new metric, using the MGD equations Eq. (3.21), Eq. (3.22). Then, we can calculate the new non-isotropic solution in two ways, both equivalent: One, we take the original EFE system Eq. (3.26-3.28) and replace the system with the new metric elements. Second, we take system Eq. (3.31-3.33), and calculate the components of θ . At the end, we implement Eq. (3.36), Eq. (3.37) and Eq. (3.38) to find the different state variables.

Having already the new state variables, we can proceed to calculate some important properties of the system, such as the Redshift $Z(r)$, sound velocity (v_t , v_r), adiabatic factor $\Gamma(r)$ and the effective mass $m(r)$

Redshift

$$Z(r) = e^{-\frac{\nu(r)}{2}} - 1. \quad (3.52)$$

Sound Velocity Components

$$v_r(r) = \left(\frac{\partial p_r}{\partial \rho} \right)^{1/2}, \quad (3.53)$$

$$v_t(r) = \left(\frac{\partial p_t}{\partial \rho} \right)^{1/2}. \quad (3.54)$$

Adiabatic Factor

Also called the Heat capacity ratio or adiabatic index. It describes the ratio of heat

capacities at constant pressure and constant volume. For stellar structures it is also called local adiabatic index (relativistic fluid), we can calculate as follows [34]:

$$\Gamma(r) = \frac{\rho(r) + p_r(r)}{p_r(r)} v_r(r). \quad (3.55)$$

Effective Mass

$$m(r) = \frac{r}{2} [1 - \mu(r)]. \quad (3.56)$$

3.2 Physical Acceptability Conditions

Up to this point, we already have a new solution obtained by means of MGD. However, the method, although proven useful, it has shown itself as just a mathematical tool to extend, and solve a system of differential equations. The physical part comes when we put this new model into test to find out if it is acceptable, and can be applied to real world phenomena. Ivanov (2017) shows the physical conditions a GR model has to fulfil in order to be considered physically admissible [35]. These are:

1.- In order to ensure a constant sign of the space-time element ds , and for rest mass to be positive. It is imperative that both metric potentials ($e^{\nu(r)}$, $e^{-\lambda(r)}$) be positive. Also, they have to be free from singularities at the center of the star ($r = 0$) [36].

$$e^{\nu(r)} > 0,$$

$$e^{-\lambda(r)} > 0.$$

At $r = 0$

$$e^{\nu(0)} = \text{constant},$$

$$e^{-\lambda(0)} = 1.$$

2.- It is very intuitive to see that state properties such as density (ρ) and components of pressure (p_r , p_t) have to be positive for $r \in [0, R]$. Moreover, at the centre ($r = 0$) they

should be finite.

$$\rho(r) > 0,$$

$$p_r(r) > 0,$$

$$p_t(r) > 0.$$

3.- The density (ρ) and components of pressure (p_r, p_t) should reach a maximum at the centre, and should decrease monotonously outwards. Furthermore, the tangential pressure is always bigger than the radial pressure, except at the center where they are equal [37].

$$\rho'(r) < 0,$$

$$p_r'(r) < 0,$$

$$p_t'(r) < 0.$$

At the centre

$$\rho'(0) = 0,$$

$$p_r'(0) = 0,$$

$$p_t'(0) = 0,$$

$$p_t(0) = p_r(0).$$

In the rest of the domain:

$$p_t(r) > p_r(r).$$

4.- One of the most important conditions are the so-called energy conditions. They ensure the energy density inside some region to be positive. They are not physical conditions "per se", but mathematical boundary constraints that approaches to the belief on positive energy [38]. Negative energy conditions are related with dark energy and matter. There are two main types the Dominant Energy Conditions (DEC) that establish the flow of mass-energy cannot be greater than light speed, and the Strong Energy Condition (SEC) that establishes matter must gravitate towards matter [39]. (Consider that this difference

is taking into account the natural units where $c=1$ and $k=1$)

DEC:

$$\rho(r) - p_r(r) > 0,$$

$$\rho(r) - p_t(r) > 0.$$

SEC:

$$\rho(r) - p_r(r) - 2p_t(r) > 0,$$

5.- There are two types of Redshift, the interior one correspondent to the one frequency-change phenomena perceived inside the stellar object. and the Surface Redshift (Z_s) (equation below) that only depends on the compactness of the star u , and refers to frequency-change phenomena perceived at the surface. They have different conditions imposed on each one. The Z_s is uniform throughout the entire surface, it depends only on u , and according to Ivanov (2002), anisotropic models has upper limits for the values of Z_s and u . When DEC holds, they are 5.211 and 0.974 respectively. When SEC holds, they are 3.842 and 0.587 [40]. Also, the Interior Redshift has to be monotonically decreasing.

Surface Redshift:

$$Z_s = (1 - 2u)^{-1/2} - 1.$$

DEC holds:

$$Z_s < 5.211,$$

$$u < 0.974.$$

SEC holds:

$$Z_s < 3.842,$$

$$u < 0.587.$$

Interior Redshift Condition:

$$Z'(r) < 0.$$

6.- The causality condition, given in the fundamentals of SR. Any speed cannot be greater than the speed of light. In this case, we are dealing with the sound speed components, acoustic waves propagating along the plasma material of the star. (Remember we set $c=1$, so velocities are fraction of this speed)

Components of Sound Speed:

$$0 < v_r < 1,$$

$$0 < v_t < 1.$$

7.- The stability against Cracking condition. The concept of cracking was introduced by Herrera (1992) [41]. He showed that this phenomena appears in a stellar object if there is an abrupt change in the radial force sign after certain value of the radius r is reached causing a non-sustainable self-gravitation object to collapse. In a more recent work Abreu (2007) [42] proposed a simple restriction. this is known as the stability region, and it fulfils:

Stability Region:

$$0 < |v_t^2 - v_r^2| < 1.$$

8.- The stability condition based on the Adiabatic Index Γ . This adiabatic index is the ratio of the heat capacities of the stellar material given a non-ideal behavior [34]. The criterion for stability by Adiabatic Index was given by Herrera [41, 43].

Stability by Adiabatic Factor:

$$\Gamma(r) > \frac{4}{3}.$$

3.3 Introducing the Andrade-Einstein solution

In the paper (Andrade-Santana, 2022), we can find a completely new physical model from the EFE, by taking a static universe in a spherically symmetric space-time, and do an isotropic extension, so the model continues to be an ideal one. Our work uses the mini-

mal geometric Transformation extended technique applied to the Einstein static universe (1915) [44], the method of finding the new solution was given by the following procedure:

First of all, we have the MGD extended method given that f and g Eq.(3.23, 3.24) (deformation functions) are non-zero:

$$\xi \mapsto \nu = \xi + \alpha g, \quad (3.57)$$

$$\mu \mapsto e^{-\lambda} = \mu + \alpha f. \quad (3.58)$$

After that, we introduce the Einstein constrains for an isotropic and static universe as the seed solution.

$$e^\nu = A, \quad (3.59)$$

$$e^{-\mu} = 1 - \frac{r^2}{C^2}, \quad (3.60)$$

$$\rho(r) = -p(r) = \frac{3}{k^2 C^2}. \quad (3.61)$$

The system we obtain consist of 9 unknowns $f(r)$, $g(r)$, e^ν , $e^{-\lambda}$, $p_r(r)$, $p_t(r)$ and the 3 theta components, but just 7 differential equations. So, we need two extra arbitrary constraints in order to close the system.

The first restriction is:

$$\theta_0^0(r) = \frac{\varrho}{k^2}. \quad (3.62)$$

The given equation set the θ_0^0 factor as constant (ϱ is a constant), so we can reach simplicity in calculations and just modifying the density by a constant factor, the restriction leads us to the following differential equation:

$$\frac{f'}{r} + \frac{f}{r^2} + \varrho = 0. \quad (3.63)$$

we solve it for $f(r)$ and get:

$$f(r) = -\frac{1}{3}\varrho r^2 + \frac{c_o}{r}. \quad (3.64)$$

In this case, we set the constant $c_o = 0$, so we can avoid singularities at $r = 0$. Now, we need another constraint, so we can close the system.

The second restriction:

$$\Pi_{\theta} = p_{\theta t} - p_{\theta r} = 0. \quad (3.65)$$

This equations tells us that we have an isotropic pressure $p = p_t = p_r$, so the solutions continues to be ideal. The second equation gives us the following differential equation for $g(r)$:

$$2r(c^2(r^2\varrho - 3) + 3r^2)g''(r) + r(c^2(r^2\varrho - 3) + 3r^2)g'(r)^2 + 6c^2g'(r) = 0. \quad (3.66)$$

We solve for $g(r)$, and we get this solution:

$$g(r) = 2\ln(2c_1(c^2\varrho + 3) + \sqrt{c^2(r^2\varrho - 3) + 3r^2}) + c_2. \quad (3.67)$$

where c_1 and c_2 are integration constants. Directly, we can find the spatial and temporal metric components, given f and g :

$$e^{\nu(r)} = B(2c_1(c^2\varrho + 3) + \sqrt{c^2(r^2\varrho - 3) + 3r^2})^2, \quad (3.68)$$

$$e^{-\lambda(r)} = 1 - \frac{r^2}{c^2} - \frac{r^2\varrho}{3}, \quad (3.69)$$

$$\rho(r) = \frac{1}{k^2} \left(\frac{3}{c^2} + \varrho \right), \quad (3.70)$$

$$p(r) = \frac{-1 + \frac{2r^2}{2c_1\sqrt{c^2(r^2\varrho-3)+3r^2} - \frac{3c^2}{c^2\varrho+3} + r^2}}{k^2r^2}. \quad (3.71)$$

As we can observe in Eq. (3.57) and Eq. (3.58), there are changes in both the spatial and temporal metrics. Normally, in the simple MGD, only the spatial metric changes, but with the introduction of the g variable, the temporal metric is affected as well. If we take a look into the constrains, this time we needed two instead of just one as usual; the first restriction taken maintained a constant density everywhere in space, and the pressure remains isotropic with the second condition. Andrade-Santana tested the physics behind the solution, and they found that the model is physically acceptable; therefore, it is an adequate choice as a seed result, so we can apply our method, and extend even more this model. In the next section we introduce anisotropy inside this ideal situation.

Chapter 4

Results and Discussion

4.1 The New Solution

In this section, we implement the MGD approach to calculate a new anisotropic solution, based on the isotropic Andrade-Einstein model, given in the previous section. It is relevant to expect an advanced result that fulfils all the physical acceptability conditions already described. In order to obtain a new model without performing complex calculations, we chose to work with the mimic constraint for pressure. The state variables p_r , p_t , ρ defined by Eqs. (3.36-3.38) and the metric functions μ, ν in Eq. (3.21-3.22) are first derived. It is important to mention, that the calculations on the different physical expressions and graphs were performed with the Software Wolfram MATHEMATICA v13.0.

From Eq. (3.68) and Eq. (3.69) we have the seed's metric elements $\mu(r)$ and $\nu(r)$. Including this expressions inside Eq. (3.32), it is easy to calculate the main function $f(r)$.

$$f(r) = -1 + \frac{1}{3}r^2 \left(\frac{3}{c^2} + \varrho \right) + \frac{1}{1 + \frac{1}{\frac{1}{2} - \frac{3c^2}{2r^2(3+c^2\varrho)} + \frac{c_1\sqrt{3r^2+c^2(-3+r^2\varrho)}}{r^2}}}. \quad (4.1)$$

Applying the matching condition Eq.(3.43) to the Andrade-Einstein model, we get the following relation equation for the constants:

$$c_1 = \frac{3\sqrt{c^2(R^2\varrho - 3) + 3R^2}}{2c^2\varrho + 6}. \quad (4.2)$$

Introducing Eq.(4.2) into Eq.(4.1) and simplifying the expression. We obtain a new form for $f(r)$

$$f(r) = \frac{r^2}{c^2} + \frac{1}{3}r^2 \left[\varrho - \frac{2(3 + c^2\varrho)}{3r^2 + c^2(-1 + r^2\varrho) - H(r)H(R)} \right]. \quad (4.3)$$

with H describing a function dependent on r .

$$H(r) = \sqrt{3r^2 + c^2(-3 + r^2\varrho)}. \quad (4.4)$$

Using Eq.(3.25) and Eq.(4.3) to find the new spatial component $\mu(r)$:

$$\mu(r) = \frac{\alpha r^2}{c^2} + \frac{1}{3}\alpha r^2 \left(\varrho - \frac{2(c^2\varrho + 3)}{-H(r)H(R) + c^2(r^2\varrho - 1) + 3r^2} \right) - \frac{r^2}{c^2} - \frac{r^2\varrho}{3} + 1. \quad (4.5)$$

Now, solving $\rho(r)$ in Eq.(3.26) from EFE, and using Eq.(4.3), we can find the effective density $\tilde{\rho}(r)$ state function.

Effective Density

$$\tilde{\rho}(r) = \frac{1 - \left[\frac{\alpha r^2}{c^2} + \frac{1}{3}\alpha r^2 \left(\varrho - \frac{2(c^2\varrho + 3)}{-H(r)H(R) + c^2(r^2\varrho - 1) + 3r^2} \right) - \frac{r^2}{c^2} - \frac{r^2\varrho}{3} + 1 \right] G(r)}{k^2 r^2}. \quad (4.6)$$

With a new function $G(r)$

$$G(r) = \left\{ \frac{r \left[P_0(r) + \frac{2}{3}\alpha r \left(\varrho - \frac{2(c^2\varrho + 3)}{-H(r)H(R) + c^2(r^2\varrho - 1) + 3r^2} \right) + \frac{2\alpha r}{c^2} - \frac{2r}{c^2} - \frac{2r\varrho}{3} \right]}{\frac{\alpha r^2}{c^2} + \frac{1}{3}\alpha r^2 \left(\varrho - \frac{2(c^2\varrho + 3)}{-H(r)H(R) + c^2(r^2\varrho - 1) + 3r^2} \right) - \frac{r^2}{c^2} - \frac{r^2\varrho}{3} + 1} + 1 \right\}, \quad (4.7)$$

$$P_0(r) = \frac{2\alpha r^2 (c^2\varrho + 3) \left(-\frac{r(c^2\varrho + 3)H(R)}{H(r)} + 2c^2 r\varrho + 6r \right)}{3(-H(r)H(R) + c^2(r^2\varrho - 1) + 3r^2)^2}. \quad (4.8)$$

From here, it is easy to calculate the radial and tangential pressures $p_r(r)$, $p_t(r)$. Taking Eq.(3.27), Eq.(3.28) and solving for $p_r(r)$, $p_t(r)$ correspondingly, we get:

Radial Pressure

$$\tilde{p}_r(r) = \frac{(\alpha - 1) (c^2 \varrho + 3) (-H(r)H(R) + c^2(H(r))^2)}{c^2 k^2 (-3H(r)H(R) + c^2(H(r))^2)}. \quad (4.9)$$

Tangential Pressure

$$\tilde{p}_t(r) = \frac{X_1(r) \left(\frac{4r^2(\varrho c^2 + 3)^2}{(H(r))^2 (H(r) - 3H(R))^2} - T(r) + \frac{4(\varrho c^2 + 3)}{(H(r))^2 - 3H(r)H(R)} + W_1(r) + X_2(r) \right)}{4k^2}, \quad (4.10)$$

$$T(r) = \frac{4 \left((\varrho H(r)r^2 + 3H(r) - 9H(R)) c^2 + 3r^2 H(r) \right) (\varrho c^2 + 3)}{(H(r))^3 (H(r) - 3H(R))^2}, \quad (4.11)$$

$$X_2(r) = \left(\frac{\alpha r^2}{c^2} + \frac{1}{3} \alpha \left(\varrho - \frac{2(\varrho c^2 + 3)}{(r^2 \varrho - 1) c^2 + 3r^2 - H(r)H(R)} \right) r^2 - \frac{\varrho r^2}{3} - \frac{r^2}{c^2} + 1 \right), \quad (4.12)$$

$$X_1(r) = \frac{2 \left(E(r) + \frac{2\alpha r}{c^2} + \frac{2}{3} \alpha \left(\varrho - \frac{2(\varrho c^2 + 3)}{(r^2 \varrho - 1) c^2 + 3r^2 - H(r)H(R)} \right) r - \frac{2\varrho r}{3} - \frac{2r}{c^2} \right)}{\frac{\alpha r^3}{c^2} + \frac{1}{3} \alpha \left(\varrho - \frac{2(\varrho c^2 + 3)}{(r^2 \varrho - 1) c^2 + 3r^2 - H(r)H(R)} \right) r^3 - \frac{\varrho r^3}{3} - \frac{r^3}{c^2} + r}, \quad (4.13)$$

$$E(r) = \frac{2\alpha (\varrho c^2 + 3) \left(2r\varrho c^2 + 6r - \frac{r(\varrho c^2 + 3)H(R)}{H(r)} \right) r^2}{3 \left((r^2 \varrho - 1) c^2 + 3r^2 - \sqrt{(r^2 \varrho - 3) c^2 + 3r^2 H(R)} \right)^2}, \quad (4.14)$$

$$W_1(r) = \frac{2rW_0(r) \left(E(r) + \frac{2\alpha r}{c^2} + \frac{2}{3} \alpha \left(\varrho - \frac{2(\varrho c^2 + 3)}{(r^2 \varrho - 1) c^2 + 3r^2 - H(r)H(R)} \right) r - \frac{2\varrho r}{3} - \frac{2r}{c^2} \right)}{\left(\frac{\alpha r^2}{c^2} + \frac{1}{3} \alpha \left(\varrho - \frac{2(\varrho c^2 + 3)}{(r^2 \varrho - 1) c^2 + 3r^2 - H(r)H(R)} \right) r^2 - \frac{\varrho r^2}{3} - \frac{r^2}{c^2} + 1 \right)}, \quad (4.15)$$

$$E(r) = \frac{2\alpha (\varrho c^2 + 3) \left(2r\varrho c^2 + 6r - \frac{r(\varrho c^2 + 3)H(R)}{H(r)} \right) r^2}{3 \left((r^2 \varrho - 1) c^2 + 3r^2 - \sqrt{(r^2 \varrho - 3) c^2 + 3r^2 H(R)} \right)^2}. \quad (4.16)$$

With $E(r)$, $W_0(r)$, $W_1(r)$, $X_1(r)$ and $X_2(r)$ being complementary functions. Once we have both components of pressure, we can find the resultant anisotropy $\Pi(r)$ of the system.

Anisotropy

$$\begin{aligned} \Pi(r) = & (r^2\alpha(3 + c^2\varrho)^2(9r^2(r^2H(r) - 8\sqrt{H(R)} + 3R^2(7H(r) - 6H(R))) + 3c^2(2r^4\varrho(H(r) \\ & - 8H(R)) + Q(r))/(3k^2H(r)(H(r) - 3H(R))^2(-3r^2 + c^2(1 - r^2\varrho) + H(r)H(R))^2(-3r^2 \\ & + c^2(3 - r^2\varrho) + 3H(r)H(R))))), \end{aligned} \quad (4.17)$$

$$\begin{aligned} Q(r) = & 81R^2(-7H(r) + H(R)) + 3r^2(-23H(r) + 35H(R) + R^2\varrho(7H(r) - 6H(R)) \\ & - 9(-28H(r) + 36H(R) + 9R^2\varrho(H(r) - H(R)))). \end{aligned} \quad (4.18)$$

with $Q(r)$ being another complementary function that helps to reduce the long form of Eq. (4.17).

In order to find a relation between constants, we need to perform the calculations considering the matching conditions Eq. (3.43-3.45). Consider an external geometry based on the classic vacuum solution given by Schwarzschild (1916). Immediately, we take a look at the first fundamental form (equating metric functions):

The First Fundamental Form(Temporal Component) is:

$$\nu(R) = 1 - \frac{2M}{R}. \quad (4.19)$$

Where $\nu(R)$ represents the temporal component of the internal metric given by Eq. (3.68), M is the Scharzschild mass, and $1 - \frac{2M}{R}$ belongs to the external metric. We solve the Eq. (4.14) for B and find.

$$B = \frac{R - 2M}{4R(c^2R^2\varrho - 3c^2 + 3R^2)}. \quad (4.20)$$

The First Fundamental Form(Radial Component) is:

$$\mu(r) = 1 - \frac{2M}{R}. \quad (4.21)$$

Where $\mu(R)$ represents the radial component of the internal metric given by Eq. (4.5), and $1 - \frac{2M}{R}$ belongs to Schwarzschild. We solve the Eq. (4.16) for ϱ and find.

$$\rho \rightarrow \frac{3(2c^2M - R^3)}{c^2R^3}. \quad (4.22)$$

The second fundamental form evaluates the radial component of the effective pressure at the surface, which must be zero.

$$\tilde{p}_r(R) = 0. \quad (4.23)$$

Eq. (4.8) shows that for p_r at $r = R$ the result is zero. Therefore, the condition is fulfilled and Eq. (4.18) becomes trivial. We can not derive any constant from it. Before continuing, it is crucial to take an additional step, and perform another transformation. In this case, we change the M constant as follows.

$$M \rightarrow uR. \quad (4.24)$$

With u representing the 'compactness' of the stellar object, defined as the mean linear density of the body. We can vary the u parameter, and find the interval for which the compactness gives us physically acceptable models, this can be done by graphical analysis.

For the next section, it is fundamental to calculate the gravitational redshift z and the adiabatic factor Γ . The sound speed components(v_r, v_t) are graphically represented only.

Redshift

$$z(r) = \frac{\sqrt{2}}{\sqrt{\frac{3\sqrt{-\frac{c^2(R-2M)}{R}}\sqrt{c^2\left(\frac{2Mr^2}{R^3}-1\right)}}{c^2} - \frac{M(r^2+9R^2)}{R^3} + 5}} - 1, \quad (4.25)$$

Adiabatic Factor

$$\Gamma(r) = \frac{c^4(2r^2R^2u - 1)F_1(uF_5 - 4)\left(F_7 + \frac{F_{12}}{F_{13}}\right)}{F_{10}\left(2r^2u\left(-55\sqrt{c^2(2u-1)} + 22\sqrt{c^2(2r^2R^2u-1)} - F_{11}\right)R^2 + F_{14}\right)\alpha}, \quad (4.26)$$

$$F_1 = \left(\sqrt{c^2(2u-1)} \sqrt{c^2(2r^2u-1)} - c^2 \left((r^2-3)u+1 \right) \right), \quad (4.27)$$

$$F_2 = \left(r^2 R^2 \sqrt{c^2(2u-1)} - \sqrt{c^2(2r^2 R^2 u - 1)} \right), \quad (4.28)$$

$$F_3 = \left(r^2 \left(\sqrt{c^2(2u-1)} - 3\sqrt{c^2(2r^2 R^2 u - 1)} \right) R^2 + 3\sqrt{c^2(2u-1)} + 7\sqrt{c^2(2r^2 R^2 u - 1)} \right), \quad (4.29)$$

$$F_4 = 108r^2 R^2 (r^2 R^2 - 1)^2 F_2 u^3 + 54 (r^2 R^2 - 1)^2 (r^2 R^2 + 1) \sqrt{c^2(2r^2 R^2 u - 1)} u^2, \quad (4.30)$$

$$F_5 = \left(F_4 + 9 (r^2 R^2 - 1) F_3 u + 22\sqrt{c^2(2u-1)} + 26\sqrt{c^2(2r^2 R^2 u - 1)} - 2r^2 R^2 \left(7\sqrt{c^2(2u-1)}, \right. \right. \\ \left. \left. + 9\sqrt{c^2(2r^2 R^2 u - 1)} \right), \quad (4.31)$$

$$F_6 = \left(\sqrt{c^2(2u-1)} + \sqrt{c^2(2r^2 R^2 u - 1)} \right), \quad (4.32)$$

$$F_7 = \frac{(r^2 - 1) u (\alpha - 1)}{c^2 ((r^2 - 3) u + 1) - \sqrt{c^2(2u-1)} \sqrt{c^2(2r^2 u - 1)}}, \quad (4.33)$$

$$F_8 = -18r^2 \left(\left(\sqrt{c^2(2r^2 u - 1)} - 2\sqrt{c^2(2u-1)} \right) r^2 + \sqrt{c^2(2r^2 u - 1)} \right) (\alpha - 1) u^2, \quad (4.34)$$

$$F_9 = \left(-28\alpha \sqrt{c^2(2u-1)} + 24\sqrt{c^2(2u-1)} + 17\alpha \sqrt{c^2(2r^2 u - 1)} - 15\sqrt{c^2(2r^2 u - 1)} \right), \quad (4.35)$$

$$F_{10} = (r^2 - 1) u \left(\sqrt{c^2(2u-1)} \sqrt{c^2(2r^2 R^2 u - 1)} - c^2 \left((r^2 R^2 - 3) u + 1 \right) \right)^2, \quad (4.36)$$

$$F_{11} = 12u \left(r^2 \left(\sqrt{c^2(2r^2 R^2 u - 1)} - 3\sqrt{c^2(2u-1)} \right) R^2 + \sqrt{c^2(2r^2 R^2 u - 1)} \right), \quad (4.37)$$

$$F_{12} = 2c^2 \left(F_8 + \left(F_9 r^2 + 9(\alpha - 1) \sqrt{c^2(2r^2 u - 1)} \right) u - 3\sqrt{c^2(2u-1)} + 6\alpha \left(\sqrt{c^2(2u-1)} \right. \right. \\ \left. \left. - \sqrt{c^2(2r^2 u - 1)} + 5\sqrt{c^2(2r^2 u - 1)} \right), \quad (4.38)$$

$$F_{13} = \sqrt{c^2(2r^2 u - 1)} \left((1 - 6r^2 u) c^2 + 3\sqrt{c^2(2u-1)} \sqrt{c^2(2r^2 u - 1)} \right)^2, \quad (4.39)$$

$$35\sqrt{c^2(2u-1)} + 30u\sqrt{c^2(2r^2 R^2 u - 1)} - 25\sqrt{c^2(2r^2 R^2 u - 1)}. \quad (4.40)$$

The $F_n(r)$ functions with $n = 1, \dots, 14$ Eq. (4.27-4.40) are also complementary functions that helps to reduce the long form of the Eq. (4.26).

4.2 Physical Analysis of the Solution

This section describes the most important part of our research in terms of physics, if a solution does not fulfil the conditions to be an acceptable physical model (Section 3.2), then the found solution would be purely mathematical. Therefore, in this segment we will test all the physical conditions given in last section by setting the value of α and varying the parameter u for compactness. It is crucial to remember, the major part of this analysis is made by taking the graphs of the state functions and properties of the system. We use a graphical analysis to determine the working interval for u by direct observation and arbitrary selection of the ones that fulfil the acceptability conditions. If we take a look at the functions we obtained before, we find hard to perform analytical calculations to get the working interval. We get a complex system of inequalities, so it is computationally intensive to do the numerical analysis of the entire system of physical conditions. Moreover, it is easier to test it just by looking at the graphs.

Temporal and radial metric components

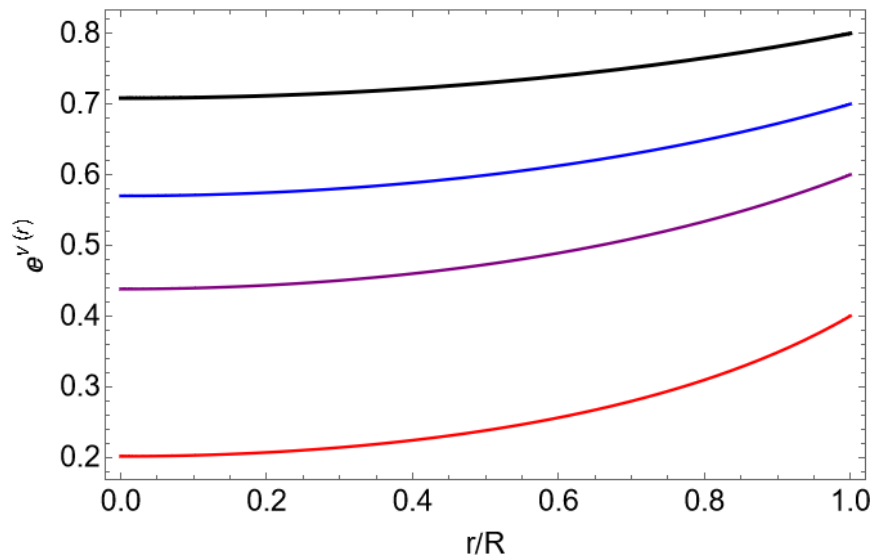


Figure 4.1: New Temporal Metric Component e^ν , $\alpha = 0.3$ for different values of compactness ($u = 0.1$ black, $u = 0.15$ blue, $u = 0.2$ red, $u = 0.3$ green)

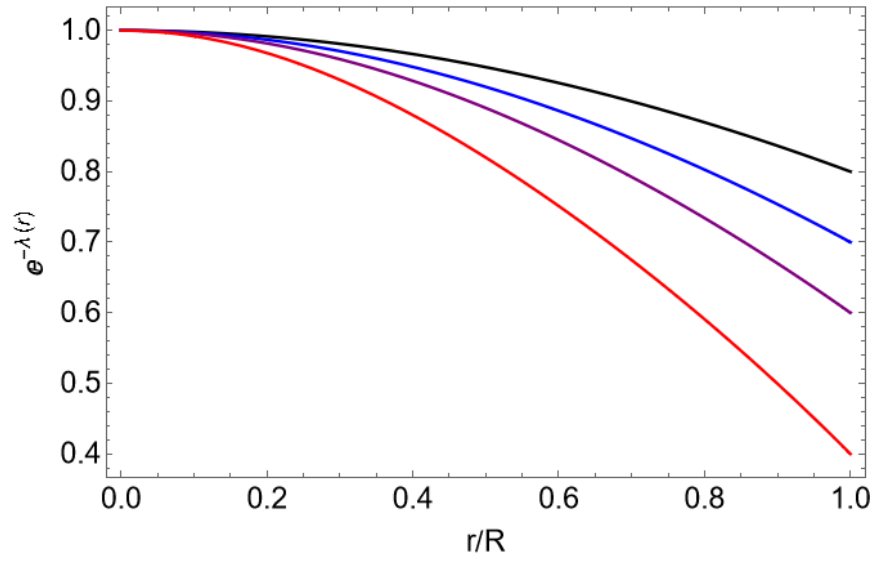


Figure 4.2: New Radial Metric Component $\mu = e^{-\lambda}$, $\alpha = 0.3$ for different values of compactness ($u = 0.1$ black, $u = 0.15$ blue, $u = 0.2$ purple, $u = 0.3$ red)

From Fig. (4.1, 4.2), we can see that they fulfil the condition of positive metric components in each point, so the signature of the metric does not change. Also, at the center of the stellar object ($r = 0$), the metric potentials fulfilled the conditions:

$$e^{\lambda(0)} = 1,$$

$$e^{\nu(0)} = \frac{1}{2} \left(-\frac{3\sqrt{c^2(2u-1)}}{\sqrt{-c^2}} - 9u + 5 \right) \text{ (positive constant).}$$

Density, Radial and Tangential Pressure

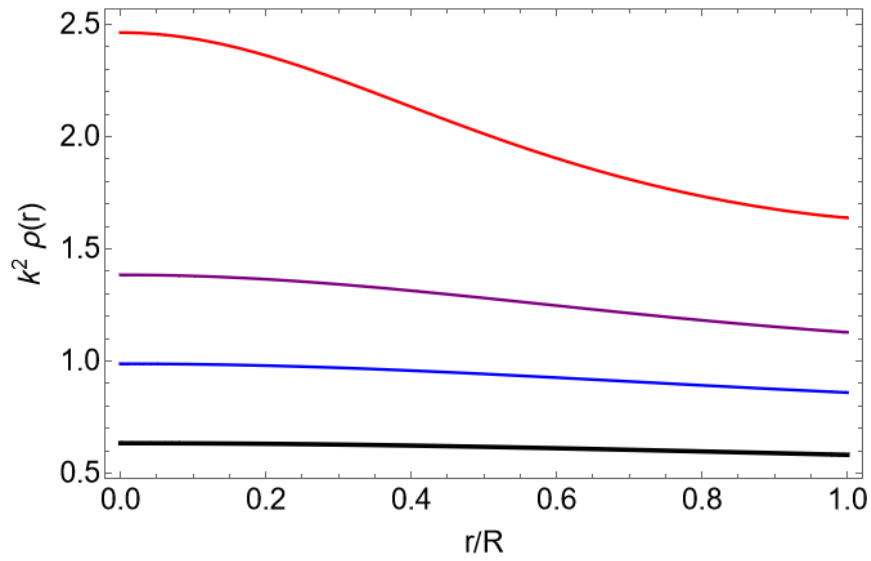


Figure 4.3: The Effective density $\tilde{\rho}$, $\alpha = 0.3$ for different values of compactness ($u = 0.1$ black, $u = 0.15$ blue, $u = 0.2$ purple, $u = 0.3$ red).

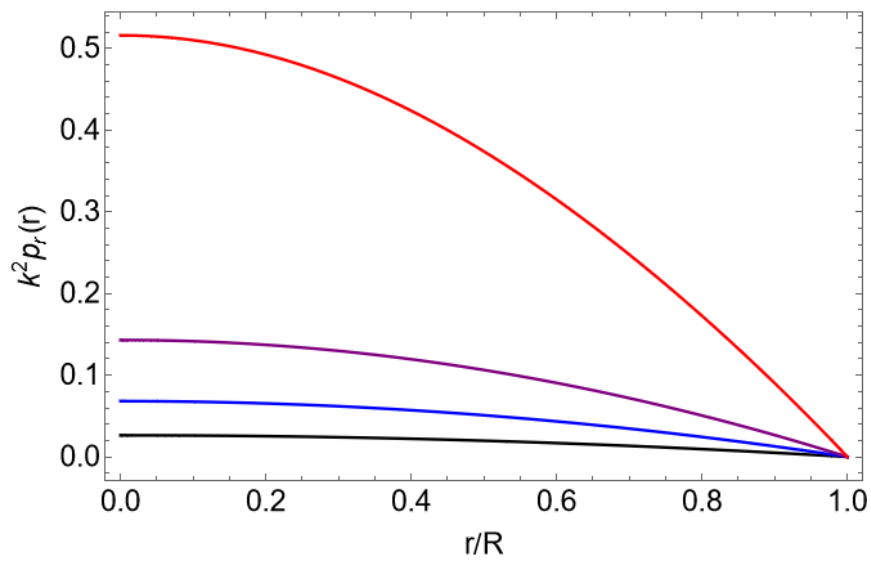


Figure 4.4: The radial component of pressure \tilde{p}_r , $\alpha = 0.3$ for different values of compactness ($u = 0.1$ black, $u = 0.15$ blue, $u = 0.2$ purple, $u = 0.3$ red).

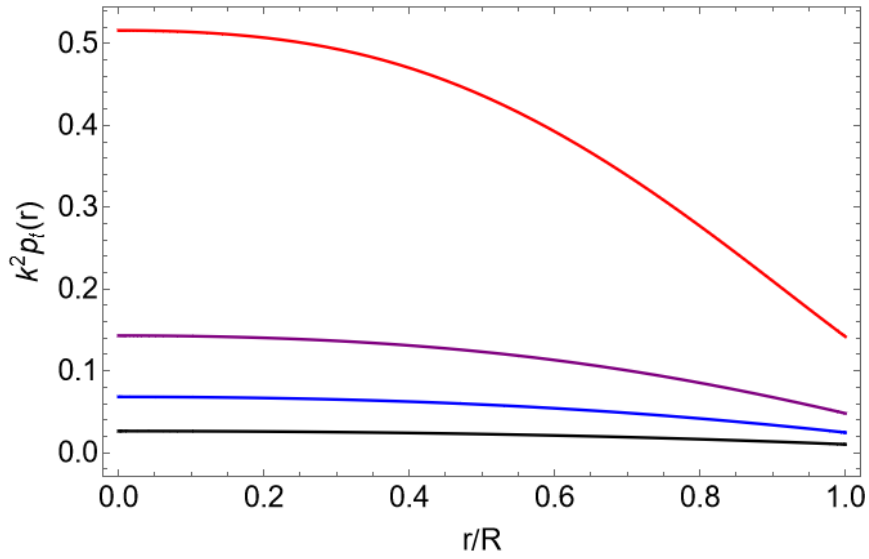


Figure 4.5: The tangential component of pressure (shear stress) \tilde{p}_t , $\alpha = 0.3$ for different values of compactness ($u = 0.1$ black, $u = 0.15$ blue, $u = 0.2$ purple, $u = 0.3$ red).

Inside the interval $r \in [0, R]$ and for a compactness interval $u \in [0.1, 0.3]$, the three graphs Fig. (4.3, 4.4, 4.5) show positiveness ($F(r) > 0$), also they are monotonically decreasing and smooth (derivable) at each point. Moreover, they present a maximum at $r = 0$ ($\tilde{\rho}'(0) = 0, \tilde{p}'_r(0) = 0, \tilde{p}'_t(0) = 0$), and both components of effective pressure are equal at $r = 0$ Eq. (4.41) (unrecognizable components at the center). They fulfil all the required physical conditions to be acceptable for the given compactness interval $u \in [0.1, 0.3]$.

$$p_t(0) = p_r(0). \quad (4.41)$$

If we want to reduce the interval for compactness u , then we have to proceed with energy conditions, so we can use the surface Redshift for getting a shorter interval. As exposed in (Section 3.2), the energy conditions are divided into two, the Dominant Energy condition (DEC) and Strong Energy Condition (SEC).

The Dominant Energy Conditions (DEC):

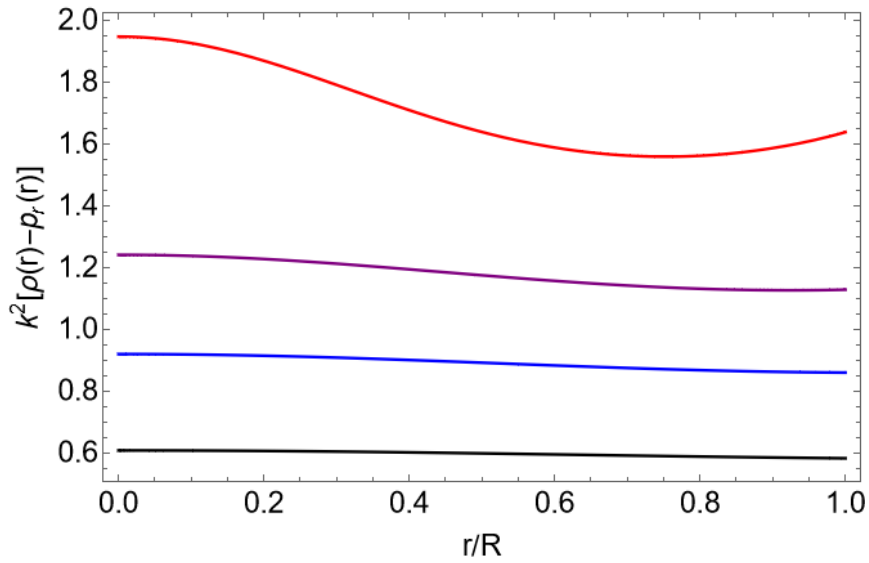


Figure 4.6: Dominant Energy Condition (DEC) for radial pressure $\rho(r) - p_r(r)$, $\alpha = 0.3$ for different values of compactness ($u = 0.1$ black, $u = 0.15$ blue, $u = 0.2$ purple, $u = 0.3$ red).

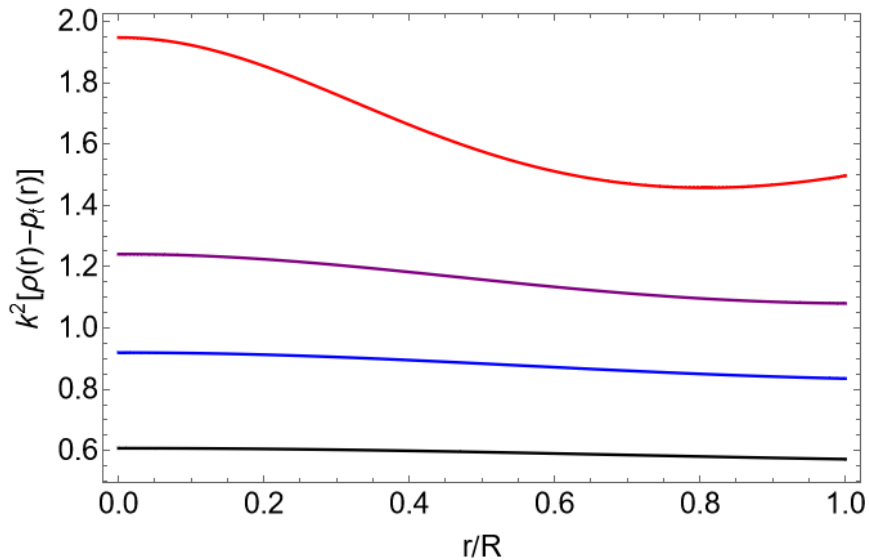


Figure 4.7: Dominant Energy Condition (DEC) for tangential pressure $\rho(r) - p_t(r)$, $\alpha = 0.3$ for different values of compactness ($u = 0.1$ black, $u = 0.15$ blue, $u = 0.2$ purple, $u = 0.3$ red).

One of the most important conditions of every GR model is the energy conditions. This ensures a positive energy inside the working interval. The dominant energy condition (DEC), as well as the Strong Energy Condition (SEC) is fulfilled in this case, making the result highly stable inside the interval $u \in [0.1, 0.3]$. $\rho(r) - p_t(r) > 0$ and $\rho(r) - p_r(r) > 0$. Figures (4.6, 4.7) shows positiveness in all cases.

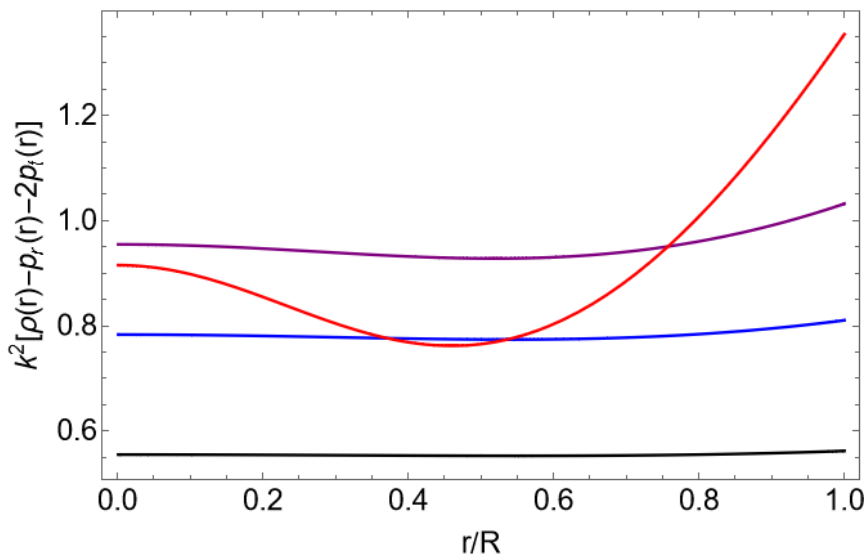
Strong Energy Condition(SEC):

Figure 4.8: The Strong Energy condition (SEC) $\rho - p_r - 2p_t$, $\alpha = 0.3$ for different values of compactness ($u = 0.1$ black, $u = 0.15$ blue, $u = 0.2$ purple, $u = 0.3$ red).

As we can see in Fig. (4.8), the SEC holds for all the compactness values. Then we can proceed to analyze the Surface Redshift.

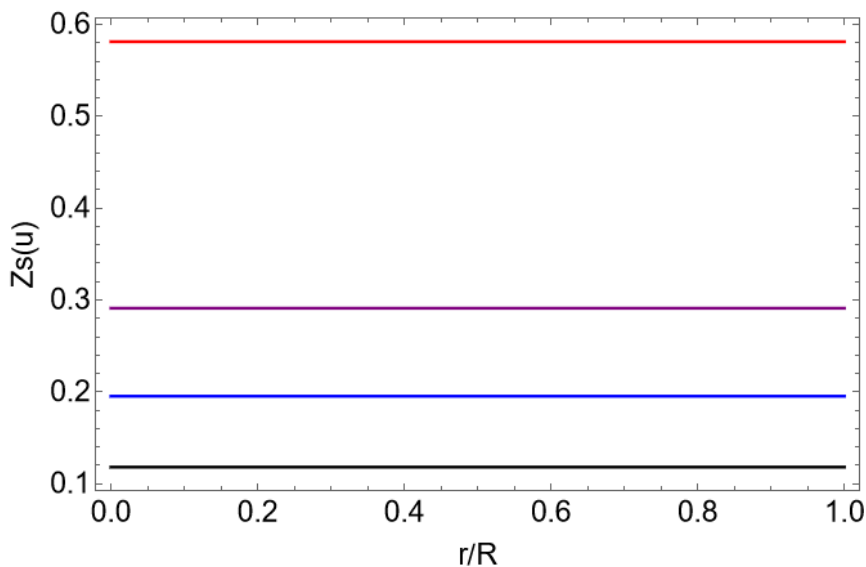
Surface Redshift

Figure 4.9: The Surface Redshift Z_s , $\alpha = 0.3$ for different values of compactness ($u = 0.1$ black, $u = 0.15$ blue, $u = 0.2$ purple, $u = 0.3$ red).

In Section (3.2) we showed the importance of Surface Redshift. One of the conditions established an upper boundary for the Z_s and for the compactness u , both dependent on

the energy conditions. As we saw in Fig. (4.8), the function fulfills the DEC and SEC. Therefore, according to information given by Ivanov (2002) [40] the limits for Z_s and u are 3.842 and 0.5785 respectively. If we take a look at Fig. (4.9), the constant lines shows that the boundaries presented are respected, so we now have found with pleasure a compactness interval to $u \in [0.1, 0.5785]$. We must continue testing more conditions in order to make this range of values shorter.

The Interior Gravitational Redshift:

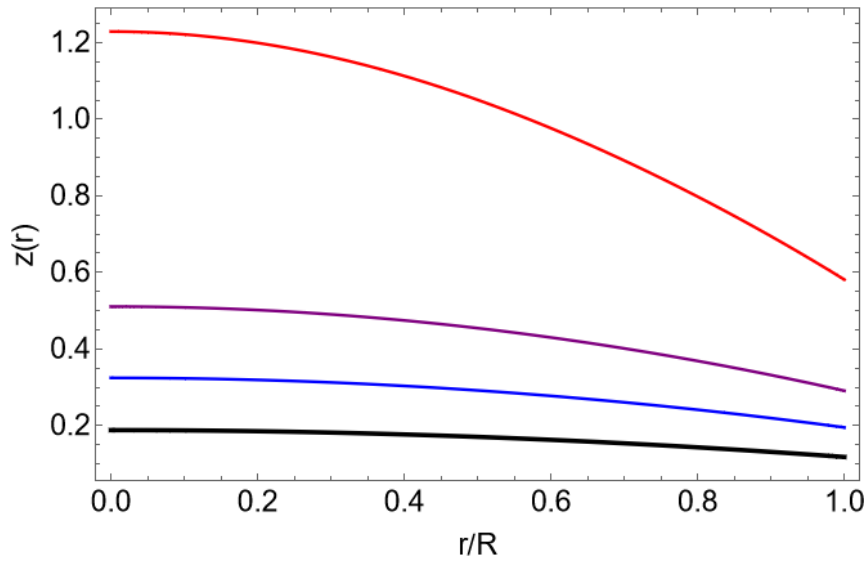


Figure 4.10: The Redshift $Z(r)$, $\alpha = 0.3$ for different values of compactness ($u = 0.1$ black, $u = 0.15$ blue, $u = 0.2$ purple, $u = 0.3$ red).

The condition imposed for Internal Redshift to be monotonically decreasing. If we take a look at Fig. (4.10), the graph shows a decreasing behavior for all the u values. So, another fulfilled condition. At this point, it is imperative to calculate the anisotropy Π to see the degree of non-ideal behavior of the fluid. We succeeded in obtaining a more realistic model (In this case we obtained a non-null shear stress given by the tangential component of pressure).

Anisotropy:

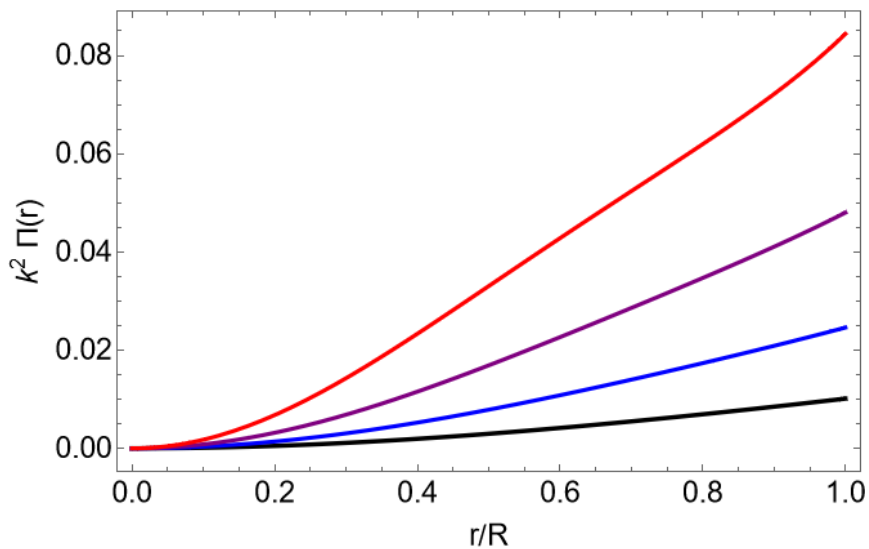


Figure 4.11: The Anisotropy of the system $\Pi = \tilde{p}_t - \tilde{p}_r$, $\alpha = 0.3$ for different values of compactness ($u = 0.1$ black, $u = 0.15$ blue, $u = 0.2$ purple, $u = 0.3$ red).

It is no surprising we got a non-isotropic model, since we postulated from the beginning the division of pressure into components. Fig. (4.11) also shows a monotonically increasing behavior.

The Sound Velocity Components:

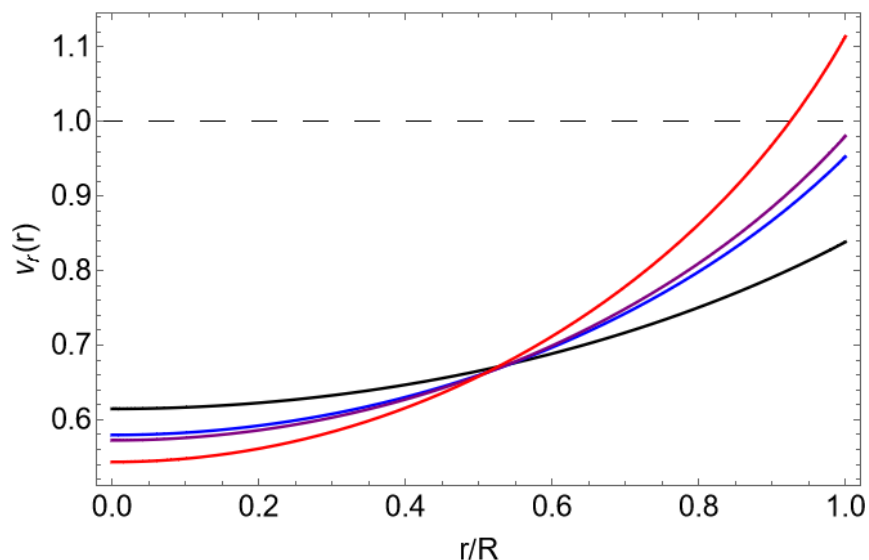


Figure 4.12: The radial component of sound speed v_r/c , $\alpha = 0.3$ for different values of compactness ($u = 0.1$ black, $u = 0.2$ blue, $u = 0.3$ purple, $u = 0.4$ red). The dashed-gray line represents the upper limit c

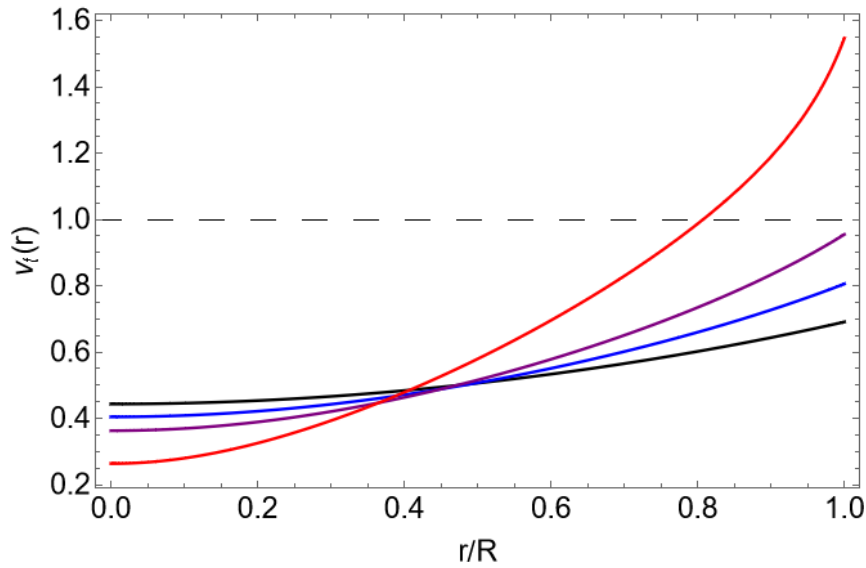


Figure 4.13: The tangential component of sound speed v_t/c , $\alpha = 0.3$ for different values of compactness ($u = 0.1$ black, $u = 0.2$ blue, $u = 0.3$ purple, $u = 0.4$ red). The dashed-gray line represents the upper limit c

One of the iconic conditions of SR is the light speed as absolute and maximum, no massive object can reach or overcome this speed. In this case, we set $c = 1$, and we graph the sound speed components as fraction of light speed. Therefore, graphs can not show velocities equal or greater than 1 at each point inside the stellar object. Fig. (4.12) shows that there is a problem when $u > 0.16$. Light speed is surpassed, so we have to discard these values of compactness. The same for Fig. (4.13), it does not fulfill the condition when $u > 0.25$. Considering the reduction on the interval, now $u \in [0.1, 0.16]$ is the best interval for an acceptable solution.

Non-Cracking Condition:

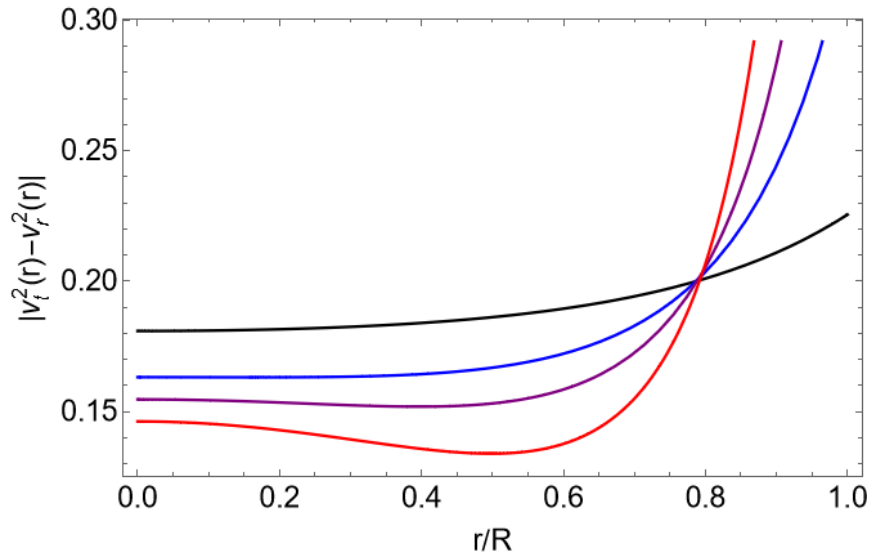


Figure 4.14: Stability against cracking $v_t^2 - v_r^2$, $\alpha = 0.3$ for different values of compactness ($u = 0.1$ black, $u = 0.15$ blue, $u = 0.2$ purple, $u = 0.3$ red).

The condition states that $0 < |v_t^2 - v_r^2| < 1$ ensures stability in convective flux of energy-matter due to the variable radial force present. In case of Figure (4.14), the graph shows for all u values the condition holds.

Adiabatic Factor:

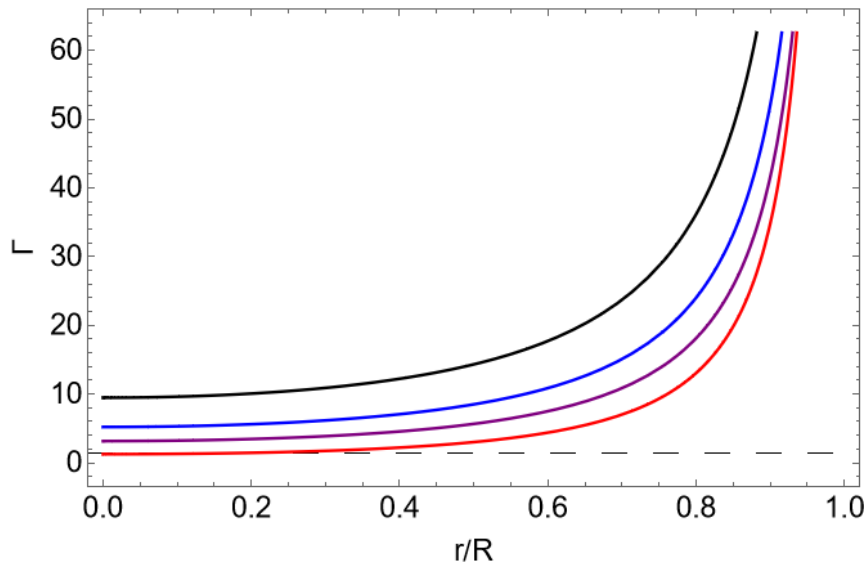


Figure 4.15: Adiabatic Factor Γ , $\alpha = 0.3$ for different values of compactness ($u = 0.1$ black, $u = 0.15$ blue, $u = 0.2$ purple, $u = 0.3$ red). The dashed-gray line represents the lower limit $\frac{4}{3}$

The condition presented for anisotropic models imposed an adiabatic factor Γ greater than the value $\frac{4}{3}$. As shown in Fig. (4.15), all the graphs fulfils the condition.

Based on what we have presented, the solution fulfilled all the conditions to be a physically acceptable model, so we can conclude that it is an applicable result for stellar structures inside the interval $u \in [0.1, 0.16]$. It is worth to mention that the value for α was kept constant due to the fact that changing the value just escalated the state functions, and did not changed the shape of these. So, there were no need to alter the value.

Chapter 5

Conclusions

General Relativity (GR) stands as a marvelous achievement within the realm of physical theories, helping scientists to elucidate one of the most fundamental forces in the cosmos: gravity. The Einstein Field Equations (EFE) are the best representation of the GR theory as it expresses the relationship between the space-time geometry and the energy-matter. Multiple solutions have been given along the last century. Unfortunately, they are characterized by the idealistic depiction of an isotropic fluid describing the energy-matter sector seconded by the spherically-symmetric geometry of space-time. However, during the last decade, a great form of introducing anisotropy into this classical solutions has appeared. The Minimal Geometric Deformation (MGD) by Gravitational Decoupling, a powerful approach that takes a previous ideal solution, and inserts a certain geometric deformation to gain a new answer, but with the particularity that this new solution is more realistic. It describes a non-perfect fluid with non-zero viscosity, thermal conduction, pressure is not isotropic anymore (anisotropy) because it now has components, the tangential component is associated with a non-null shear stress on the fluid [7]. By means of this method, and using a recent result, the so-called Andrade-Einstein solution [44], we obtained a new non-perfect solution. The outcome model was tested to see if it is a physically acceptable solution [35]. In order to see the acceptability, we resort to graphical analysis performed in the last part of chapter 4, due to the high complexity in solving a system of inequalities that involve extensive functions (see previous chapter). Therefore, multiple graphs on each physical conditions were displayed and investigated. The anisotropy was calculated and showed in one of the graphs, so we can prove that solution given by Eq. (4.3), Eq. (4.5),

Eq. (4.6), Eq. (4.8), Eq. (4.9) and Eq. (4.13) is non-ideal. Finally, results in each one of the graphs showed satisfactorily that the solution fulfilled all the physical requirements (Section 3.2). Thence, we have obtained a new tested stellar model working on the compactness interval $u \in [0.1, 0.16]$ for $\alpha = 0.3$ (Other values of α would have just escalated the graphs, and there will be no appreciable change). It is important to remark, this method has many weak points. One of them is the constraints that we have to consider in order to complete the system of equations, another one is the matching conditions in which the vacuum solution arbitrary selected as our external metric due to the fact that it is easy to work with, but the main problem is that it does not fully represent the external geometry of the environment around self-gravitational stellar objects. Furthermore, the method requires graphical analysis for checking the fulfillment of physical conditions, which is also a problem because we have to adjust the parameters α and compactness u in order to find the "best" values that fulfils all the conditions.

The MGD method has some failures, but it is an excellent modern method that has been changing last decade, so we can apply more efficiently distinct models without losing too much rigor. It is an approach that needs more analysis and more attention. It is crucial to remind that this is one of the few methods to find an exact solution to the EFE. I encourage to continue the development of this technique.

Bibliography

- [1] B. Schutz, *A First Course in General Relativity*, 2nd ed. Cambridge University Press, Jun. 2009. [Online]. Available: <http://www.worldcat.org/isbn/0521887054>
- [2] G. M. Clemence, “The relativity effect in planetary motions,” *Rev. Mod. Phys.*, vol. 19, pp. 361–364, Oct 1947. [Online]. Available: <https://link.aps.org/doi/10.1103/RevModPhys.19.361>
- [3] D. W. Castelvechi, “A. einstein’s gravitational waves found at last,” *Nature*, 2016.
- [4] K. Schwarzschild, “Über das Gravitationsfeld eines Massenpunktes nach der Einsteinschen Theorie,” *Sitzungsberichte der Königlich Preussischen Akademie der Wissenschaften*, pp. 189–196, Jan. 1916.
- [5] R. C. Tolman, “Static solutions of einstein’s field equations for spheres of fluid,” *Phys. Rev.*, vol. 55, pp. 364–373, Feb 1939. [Online]. Available: <https://link.aps.org/doi/10.1103/PhysRev.55.364>
- [6] R. Meyers, *Encyclopedia of Physical Science and Technology*, ser. Encyclopedia of Physical Science and Technology. Academic Press, 2002, no. v. 12. [Online]. Available: <https://books.google.com.ec/books?id=lo1UAAAAMAAJ>
- [7] J. Ovalle, R. Casadio, R. da Rocha, and A. Sotomayor, “Anisotropic solutions by gravitational decoupling,” *The European Physical Journal C*, vol. 78, no. 2, feb 2018. [Online]. Available: <https://doi.org/10.1140%2Fepjc%2Fs10052-018-5606-6>
- [8] R. H. Dicke, “New research on old gravitation,” *Science*, vol. 129, no. 3349, pp. 621–624, 1959. [Online]. Available: <http://www.jstor.org/stable/1758172>

- [9] S. Carroll, *Spacetime and Geometry: An Introduction to General Relativity*. Benjamin Cummings, 2003. [Online]. Available: <http://www.amazon.com/Spacetime-Geometry-Introduction-General-Relativity/dp/0805387323>
- [10] F. Dillen and L. Verstraelen, *Handbook of Differential Geometry*. Elsevier Science, 2005. [Online]. Available: <https://books.google.com.ec/books?id=QUuLp4W1bFAC>
- [11] J. Lee, *Introduction to Riemannian Manifolds*, ser. Graduate Texts in Mathematics. Springer International Publishing, 2019. [Online]. Available: <https://books.google.com.ec/books?id=UIPltQEACAAJ>
- [12] L. D. Landau and E. M. Lifshitz, *The Classical Theory of Fields*, 4th ed. Butterworth-Heinemann, Jan. 1980. [Online]. Available: <http://www.worldcat.org/isbn/0750627689>
- [13] W. Boothby, *An Introduction to Differentiable Manifolds and Riemannian Geometry, Revised*, ser. Pure and Applied Mathematics. Elsevier Science, 2003. [Online]. Available: <https://books.google.com.ec/books?id=DFYs99E-IFYC>
- [14] C. W. Misner, K. S. Thorne, and J. A. Wheeler, *Gravitation*, Misner, C. W., Thorne, K. S., & Wheeler, J. A., Ed., 1973.
- [15] J. Foster and J. Nightingale, *A Short Course in General Relativity*. Longman, 1995. [Online]. Available: <https://books.google.com.ec/books?id=8qQPAQAAMAAJ>
- [16] A. Einstein, “On the electrodynamics of moving bodies,” *Annalen der Physik*, vol. 17, pp. 891–921, 1905.
- [17] S. Chowdhury and T. Sarkar, “Small anisotropy in stellar objects in modified theories of gravity,” *The Astrophysical Journal*, vol. 884, no. 1, p. 95, oct 2019. [Online]. Available: <https://doi.org/10.3847%2F1538-4357%2F19080109>
- [18] J. Ovalle, R. Casadio, and A. Sotomayor, “The minimal geometric deformation approach: A brief introduction,” *Advances in High Energy Physics*, vol. 2017, pp. 1–9, 2017. [Online]. Available: <https://doi.org/10.1155%2F2017%2F9756914>

- [19] R. Casadio, J. Ovalle, and R. da Rocha, “The minimal geometric deformation approach extended,” *Classical and Quantum Gravity*, vol. 32, no. 21, p. 215020, oct 2015. [Online]. Available: <https://doi.org/10.1088%2F0264-9381%2F32%2F21%2F215020>
- [20] J. Ovalle, “Extending the geometric deformation: New black hole solutions,” *International Journal of Modern Physics: Conference Series*, vol. 41, p. 1660132, jan 2016. [Online]. Available: <https://doi.org/10.1142%2Fs2010194516601320>
- [21] R. Casadio and J. Ovalle, “Brane-world stars and (microscopic) black holes,” *Physics Letters B*, vol. 715, no. 1-3, pp. 251–255, aug 2012. [Online]. Available: <https://doi.org/10.1016%2Fj.physletb.2012.07.041>
- [22] J. Ovalle and F. Linares, “Tolman IV solution in the randall-sundrum braneworld,” *Physical Review D*, vol. 88, no. 10, nov 2013. [Online]. Available: <https://doi.org/10.1103%2Fphysrevd.88.104026>
- [23] K. Lake, “All static spherically symmetric perfect-fluid solutions of einstein’s equations,” *Physical Review D*, vol. 67, no. 10, may 2003. [Online]. Available: <https://doi.org/10.1103%2Fphysrevd.67.104015>
- [24] S. K. Maurya and M. Govender, “A family of charged compact objects with anisotropic pressure,” *The European Physical Journal C*, vol. 77, no. 6, jun 2017. [Online]. Available: <https://doi.org/10.1140%2Fepjc%2Fs10052-017-4982-7>
- [25] F. E. Schunck and E. W. Mielke, “General relativistic boson stars,” *Classical and Quantum Gravity*, vol. 20, no. 20, pp. R301–R356, sep 2003. [Online]. Available: <https://doi.org/10.1088%2F0264-9381%2F20%2F20%2F201>
- [26] V. Dzhunushaliev, V. Folomeev, R. Myrzakulov, and D. Singleton, “Non-singular solutions to einstein-klein-gordon equations with a phantom scalar field,” *Journal of High Energy Physics*, vol. 2008, no. 07, pp. 094–094, jul 2008. [Online]. Available: <https://doi.org/10.1088%2F1126-6708%2F2008%2F07%2F094>

- [27] H. Lü, A. Perkins, C. Pope, and K. Stelle, “Black holes in higher derivative gravity,” *Physical Review Letters*, vol. 114, no. 17, apr 2015. [Online]. Available: <https://doi.org/10.1103/PhysRevLett.114.171601>
- [28] A. D. Felice and S. Tsujikawa, “f(r) theories,” *Living Reviews in Relativity*, vol. 13, no. 1, jun 2010. [Online]. Available: <https://doi.org/10.12942/lrr-2010-3>
- [29] T. P. Sotiriou and V. Faraoni, “
$$\text{mml:math xmlns:mml=} \text{http://www.w3.org/1998/math/MathML} \text{ display="inline" mml:mrow mml:mif/mml:mimml:mrow mml:mo(/mml:momml:mir/mml:mimml:} \text{of gravity,}” *Reviews of Modern Physics*, vol. 82, no. 1, pp. 451–497, mar 2010. [Online]. Available: <https://doi.org/10.1103/RevModPhys.82.451>$$
- [30] L. Herrera and N. Santos, “Local anisotropy in self-gravitating systems,” *Physics Reports*, vol. 286, no. 2, pp. 53–130, 1997. [Online]. Available: <https://www.sciencedirect.com/science/article/pii/S0370157396000427>
- [31] W. Israel, “Singular hypersurfaces and thin shells in general relativity.” *Il Nuovo Cimento B (1965-1970)*, 1966.
- [32] J. Ovalle, E. Contreras, and Z. Stuchlik, “Energy exchange between relativistic fluids: the polytropic case,” *The European Physical Journal C*, vol. 82, no. 3, mar 2022. [Online]. Available: <https://doi.org/10.1140/epjc/s10052-022-10168-5>
- [33] L. Herrera, “Complexity and simplicity of self-gravitating fluids,” 2023.
- [34] W. Stolzmann and T. Blöcker, “A semirelativistic equation of state for stellar interiors,” *Contributions to Plasma Physics*, vol. 39, no. 1-2, pp. 105–108, jan 1999. [Online]. Available: <https://doi.org/10.1002/ctpp.2150390126>
- [35] B. V. Ivanov, “Analytical study of anisotropic compact star models,” *The European Physical Journal C*, vol. 77, no. 11, nov 2017. [Online]. Available: <https://doi.org/10.1140/epjc/s10052-017-5322-7>
- [36] S. K. Maurya, S. D. Maharaj, and D. Deb, “Generalized anisotropic models for conformal symmetry,” *European Physical Journal C*, vol. 79, no. 2, p. 170, Feb. 2019.

- [37] G. G. L. Nashed and S. Capozziello, “Stable and self-consistent compact star models in teleparallel gravity,” *The European Physical Journal C*, vol. 80, no. 10, oct 2020. [Online]. Available: <https://doi.org/10.1140%2Fepjc%2Fs10052-020-08551-1>
- [38] E.-A. Kontou and K. Sanders, “Energy conditions in general relativity and quantum field theory,” *Classical and Quantum Gravity*, vol. 37, no. 19, p. 193001, sep 2020. [Online]. Available: <https://doi.org/10.1088%2F1361-6382%2Fab8fcf>
- [39] H. Maeda and T. Harada, “Criteria for energy conditions,” *Classical and Quantum Gravity*, vol. 39, no. 19, p. 195002, aug 2022. [Online]. Available: <https://doi.org/10.1088%2F1361-6382%2Fac8861>
- [40] B. V. Ivanov, “Static charged perfect fluid spheres in general relativity,” *Physical Review D*, vol. 65, no. 10, apr 2002. [Online]. Available: <https://doi.org/10.1103%2Fphysrevd.65.104001>
- [41] L. Herrera, “Cracking of self-gravitating compact objects,” *Physics Letters A*, vol. 165, no. 3, pp. 206–210, 1992. [Online]. Available: <https://www.sciencedirect.com/science/article/pii/037596019290036L>
- [42] H. Abreu, H. Hernández, and L. A. Núñez, “Sound speeds, cracking and the stability of self-gravitating anisotropic compact objects,” *Classical and Quantum Gravity*, vol. 24, no. 18, pp. 4631–4645, aug 2007. [Online]. Available: <https://doi.org/10.1088%2F0264-9381%2F24%2F18%2F005>
- [43] A. Di Prisco, L. Herrera, and V. Varela, “Cracking of homogeneous self-gravitating compact objects induced by fluctuations of local anisotropy,” *General Relativity and Gravitation*, vol. 29, 10 1997.
- [44] J. C. Andrade Landeta and D. Santana, “An isotropic extension of einstein’s universe solution through gravitational decoupling,” *European Physical Journal C*, vol. 83, 11 2022.